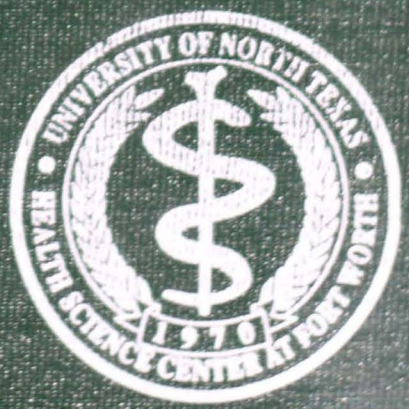
UNIVERSITY OF NORTH TEXAS
HEALTH SCIENCE CENTER AT FORT WORTH
1970

ABSTRACT

The 5-Hydroxytryptamine$_3$ (the 5-HT$_3$) receptor is composed of homomers of A subunits or heteromers of A and B subunits. The discovery of the crystal structure of the acetylcholine binding protein (Brejc et al., 2001) has helped us identify the generalized structure of the N-terminal domains of this superfamily, but the precise details regarding the amino acid residues involved in the process of ligand binding in the 5-HT$_3$ receptor are unknown.

Mouse and human 5-HT$_{3A}$ receptors are 84% identical at the amino acid level, yet they have differential sensitivities to numerous drugs that bind to the ligand recognition site, for example, agonists such as 2-Methyl serotonin and *m*-Chlorophenyl Biguanide (*m*-CPBG) and competitive antagonists such as d-Tubocurarine (curare).

The distal 1/3 part of the N-terminal domain, which contains both Loop C and Loop F is responsible for determining the potency of curare for the 5-HT$_{3A}$ receptor, these loops consist of thirteen non-conserved amino acid residues between mouse and human the 5-HT$_{3A}$ receptors. As a result of these differences, curare is 135-fold more potent at the mouse wild-type receptor than human wild-type receptor.

In this project we utilized the differential curare sensitivity of mouse and human 5-HT$_{3A}$ receptors to obtain information regarding the amino acid residues in Loop C, involved in ligand binding process. Chimeric and point mutant receptors were

constructed on the human receptor background with substitutions of corresponding mouse orthologs and expressed in *Xenopus* oocytes. Curare potency was assessed with two-electrode voltage clamp electrophysiological recordings. Our results suggests that a minimum of four mouse orthologs are required to produce the curare IC_{50} of 41 nM obtained in the chimeric receptor, which contains seven mouse orthologs (Hch Loop C receptor).

THE ROLE OF LOOP C OF THE 5-HYDROXYTRYPTAMINE$_{3A}$ RECEPTOR IN LIGAND RECOGNITION

RASHMI R. LOTE

APPROVED:

Major Professor

Committee Member

Committee Member

University Member

Chair, Department of Biomedical Sciences

Dean, Graduate School of Biomedical Sciences

The role of Loop C of the 5-Hydroxytryptamine$_{3A}$ receptor in ligand recognition.

Master's Thesis

Submitted by
Rashmi R. Lote

Advised by

Dr. Tina K. Machu

ACKNOWLEDGEMENT

I would like to express my thankfulness to my adviser, Dr. Tina K. Machu, for her support in this project. I thank Dr. Singh and Dr. Dillon for serving on my committee and their good advice. I also thank Dr. Patricia Gwirtz for being the university member on my committee.

I thank my husband, my brother and my parents for their constant support and encouragement.

Finally I thank all my colleagues in Dr. Machu's lab for their help.

TABLE OF CONTENTS

I. INTRODUCTION **1**

A. 5-HT_3 RECEPTOR: A LIGAND GATED ION CHANNEL 1
B. RECEPTOR STRUCTURE, ASSEMBLY AND TRAFFICKING 2
C. 5-HT_3 RECEPTOR SUBTYPES, HOMOMERIC VS. HETEROMERIC RECEPTORS 5
D. THE LIGAND BINDING DOMAINS OF THE 5-HT_3 RECEPTOR 7
E. INTERSPECIES STUDIES 14
F. GATING 18
G. GAPS IN OUR KNOWLEDGE 21
H. HYPOTHESIS 22

II. MATERIAL AND METHODS **24**

A. REAGENTS 24
B. CONSTRUCTION OF CHIMERIC 5-HT_{3A} RECEPTORS 25
C. SITE DIRECTED MUTAGENESIS 27
D. CESIUM CHLORIDE GRADIENT PURIFICATION OF cDNA 34
E. IN VITRO TRANSCRIPTION 36
F. PREPARATION AND MAINTENANCE OF *XENOPUS* OOCYTES 37
G. MICROINJECTION OF *XENOPUS* OOCYTES WITH RECEPTOR cRNA 38
H. ELECTROPHYSIOLOGICAL RECORDINGS OF THE 5-HT_{3A} RECEPTOR RESPONSES 38
I. DATA ANALYSIS 39

III. RESULTS **41**

A. CHARACTERIZATION OF 5-HT RESPONSE CURVES IN HUMAN CHIMERIC 5-HT_{3A} RECEPTORS AND HETEROMERIC HUMAN AND MOUSE 5-$HT_{3A/B}$ RECEPTORS 44
B. CURARE POTENCIES OF CHIMERIC HUMAN 5-HT_3 RECEPTORS 47
1. E224D mutation in the H-2/3 Loop C receptor is essential for generating the curare IC_{50} of 34 nM. *47*
2. All four mutations present in 2/3 Loop C receptor are essential. *49*
3. The interaction of R219K and V237I do not enhance the curare potency. *51*
4. The differential curare sensitivity of heteromeric human and mouse (5-$HT_{3A/B}$) receptors. *53*

IV. DISCUSSION **57**

V. REFERENCES: **67**

LIST OF FIGURES

FIGURE 1 OVERALL STRUCTURE OF $5HT_{3A}$ RECEPTOR. THE RECEPTOR HAS FIVE SUBUNITS, EACH SUBUNIT CONSISTS OF LARGE EXTRACELLULAR N-TERMINUS, FOUR TRANSMEMBRANE DOMAINS AND SHORT EXTRACELLULAR C-TERMINUS. 3
FIGURE 2 POSITION OF LIGAND BINDING SITES IN THE HOMOMERIC $5\text{-}HT_3$ RECEPTORS. EACH RECEPTOR HAS TWO LIGAND BINDING SITES LOCATED ALTERNATELY ON THE SUBUNIT INTERFACE. THE SUBUNIT INTERFACE IS FORMED OF PRINCIPAL FACE (RED) OF ONE SUBUNIT AND COMPLEMENTARY FACE (BLUE) FROM ANOTHER SUBUNIT..... 7
FIGURE 3 MOLECULAR MODEL FOR THE LIGAND-BINDING SITE OF $5\text{-}HT_{3A}$ RECEPTOR. LEFT SIDE REPRESENTS PRINCIPAL FACE WITH LOOP A (RED), B (SKY BLUE) AND C (ORANGE). RIGHT SIDE REPRESENTS COMPLEMENTARY FACE WITH LOOP D (MAGENTA), E (YELLOW) AND F (GREEN), (YAN AND WHITE, 2005)..... 8
FIGURE 4 HOMOLOGY MODEL OF LIGAND BINDING SITE OF $5\text{-}HT_{3A}$ RECEPTOR. THE DARK GRAY AREA REPRESENTS + (PRINCIPAL) FACE AND THE LIGHT GRAY AREA REPRESENTS – (COMPLEMENTARY) FACE. THE ARROW REPRESENTS ENTRY OF CURARE MOLECULE IN THE BINDING POCKET (MAKSAY ET AL, 2003). 13
FIGURE 5 STRUCTURE OF *D*-TUBOCURARINE (YAN ET AL., 2002)..... 16
FIGURE 6 THE HUMAN CHIMERIC $5\text{-}HT_{3A}$ RECEPTOR CDNAS USED IN THE PRESENT STUDY WERE GENERATED BY SUBSTITUTION OF NUCLEOTIDES ENCODING NON-CONSERVED RESIDUES IN LOOP C WITH THAT OF MOUSE RECEPTOR CDNA. 25
FIGURE 7 A HUMAN CHIMERA CONTAINING SIX OF SEVEN MUTATIONS IN LOOP C (V237 WAS NOT MUTATED), HCH-217->228, AND H-2/3 LOOP C (217,223,224,228) HAD THE SAME CURARE POTENCY AS HCH-LOOP C. 43
FIGURE 8 CURARE CONCENTRATION RESPONSE CURVES WERE PERFORMED IN HUMAN $5\text{-}HT_{3A}$ RECEPTORS CONTAINING POINT MUTANT MOUSE ORTHOLOGS IN LOOP C. NONE OF THE POINT MUTANT RECEPTORS REDUCED THE CURARE IC_{50} TO THAT OF THE HUMAN LOOP C CHIMERIC RECEPTOR (HCH LOOP C RECEPTOR). 44
FIGURE 9 SEROTONIN RESPONSE CURVES FOR CHIMERIC $5HT_{3A}$ RECEPTORS ON HUMAN BACKGROUND. 46
FIGURE 10 SEROTONIN RESPONSE CURVES FOR THE WILD TYPE MOUSE AND HUMAN HETEROMERIC RECEPTORS ($5HT_{3A/B}$ RECEPTORS). 47
FIGURE 11 CURARE INHIBITION RESPONSE CURVES FOR H-Y217Q, R219K, M223I, Y228S AND H-Y217Q, R219K, M223I, S225I, Y228S. NO SIGNIFICANT DIFFERENCE WAS FOUND IN THE CURARE IC_{50}S OF THESE TWO RECEPTORS (STUDENT'S T-TEST, P=0.90). 49
FIGURE 12 CURARE INHIBITION RESPONSE CURVES FOR CHIMERIC RECEPTORS ON HUMAN BACKGROUND, EACH OF WHICH CONTAINS A DIFFERENT PERMUTATION OF TWO OR THREE MUTATIONS FROM H-2/3 LOOP C RECEPTOR. NONE OF THESE RECEPTORS COULD MIMIC THE CURARE POTENCY OF H-2/3 LOOP C RECEPTOR..... 51

FIGURE 13 CURARE INHIBITION RESPONSE CURVES FOR H-2/3 LOOP C RECEPTOR, H-R219K, V237I AND H-Y217Q, R219K, M223I, Y228S, V237I. ONE-WAY ANOVA OF IC_{50}S WAS SIGNIFICANTLY DIFFERENT, $F_{(2,44)} = 1079.2$, $P < 0.0001$; $^{*}P < 0.05$, $^{+}P < 0.001$ COMPARED TO H-2/3 LOOP C, TUKEY-KRAMER POST-HOC TEST. THE INTERACTION OF R219K AND V237I DO NOT SHOW ANY ENHANCEMENT IN THE CURARE POTENCY. 53
FIGURE 14 PICROTOXIN INHIBITION IN HOMOMERIC AND HETEROMERIC MOUSE $5HT_3$ RECEPTORS, (STUDENT'S PAIRED T-TEST, P, < 0.05). MWT_A RECEPTOR SHOWS GREATER % INHIBITION AT 250 AND 500 μM PICROTOXIN COMPARED TO THE MWT_{A+B} RECEPTOR..... 55
FIGURE 15 CURARE INHIBITION RESPONSE CURVES FOR HETEROMERIC HUMAN AND MOUSE RECEPTORS ($5HT_{3A/B}$). HETEROMERIC MOUSE $5HT_{3A/B}$ RECEPTOR SHOWS APPROXIMATELY 100-FOLD HIGHER CURARE POTENCY AS COMPARED TO THE HETEROMERIC HUMAN $5HT_{3A/B}$ RECEPTOR. 56
FIGURE 16 THE SEQUENTIAL ALIGNMENT OF CDNAS ENCODING THE 5-HT3A RECEPTOR SUBUNITS THAT HAVE BEEN CLONED FROM FERRET, HUMAN, RAT AND MOUSE. THE E/D RESIDUES, WHICH CORRESPOND TO THE CRITICAL E224, ARE SHOWN IN GREEN. 63
FIGURE 17 SUMMARY OF THE ROLES OF AMINO ACID RESIDUES PRESENT IN LOOP C OF THE $5\text{-}HT_{3A}$ RECEPTOR, IN THE PROCESS OF LIGAND BINDING. 65

LIST OF TABLES

TABLE 1 PRIMERS USED FOR CONSTRUCTION OF CHIMERIC RECEPTORS BY SITE-DIRECTED MUTAGENESIS. 29
TABLE 2 CYCLING PARAMETERS FOR THE QUIKCHANGE SITE-DIRECTED MUTAGENESIS METHOD. 30
TABLE 3 SUMMARY OF THE 5-HT CONCENTRATION RESPONSE CURVES SHOWING EC_{50s} AND HILL COEFFICIENTS FOR WILD TYPE AND CHIMERIC 5-HT_3 RECEPTORS..... 46

I. INTRODUCTION

A. 5-HT_3 Receptor: a ligand gated ion channel

Serotonin (5-hydroxytryptamine) is a biogenic amine neurotransmitter, which mediates many central and peripheral nervous system functions by its interaction with specific 5-HT receptors. The actions of 5-HT include modulation of neuronal, muscular, endocrine and immune systems. To date at least sixteen different 5-HT receptor (5-HTR) subtypes have been identified through molecular cloning, physiological and pharmacological studies. These 5-HT receptors are classified on the basis of transductional (receptor coupling) and structural (gene structure and primary amino acid sequence) characteristics. The sixteen 5-HT receptors are classified as 5-HT_1, 5-HT_2, 5-HT_3, 5-HT_4, 5-HT_5, 5-HT_6, and 5-HT_7, each of which may have a number of subclasses (A, B, C etc.). Except the 5-HT_3 receptor, all other 5-HT receptors are metabotropic, i.e. these receptors interact with G proteins and mediate their effects via second messenger signaling system. The 5-HT_3 receptor on the other hand is a ligand gated ion channel (reviewed in Reeves and Lummis, 2002).

The 5-HT_3 receptor is a member of the superfamily of ligand gated ion channels (LGIC), of which the nicotinic acetylcholine receptor (nAChR) is the prototype. The other two members of this family are GABA receptor and glycine receptors (Corringer et al., 2000, Reeves et al., 2001; Karlin et al., 2002). The nACh receptor and 5-HT_3

receptors are cation selective while GABA receptor and glycine receptors are anion selective (Peters et al., 2005). The 5-HT_3 receptor mediates fast synaptic transmission conducting primarily Na^+ and K^+ and to a lesser extent Ca^{2+}. The highest number of 5-HT_3 receptor-binding sites in the central nervous system occurs in the area postrema and solitary tract nucleus (Gehlert et al., 1991). In addition, a large number of 5-HT_3 receptors are found in the peripheral nervous system and gut (Tyers et al., 1991). The most well documented actions of 5-HT_3 receptors are to alter gastrointestinal motility and to regulate vomiting reflex (Aapro et al., 1991). Moreover, the 5-HT_3 receptor has been implicated in altering the voluntary intake of ethanol in humans (Johnson et al., 1993; Johnson et al., 2000; Swift et al., 1996) and rodents (Knapp and Pohorekcky, 1992).

B. Receptor Structure, Assembly and Trafficking

The 5-HT_3 receptor has an oligopentameric structure, similar to that of the structure of nACh receptor. Electron microscopy of the affinity purified 5-HT_3 receptor, has shown that the five subunits are arranged around a long cylindrical axis of 11 nM and the external diameter of the ion channel is 8 nM. The ion channel opens at the external side of the cell wall and the diameter of the open channel is 2-3 nM (Boess et al., 1992; Boess et al 1995). Hydropathy plots of deduced amino acid sequences of these receptor subunits suggest a putative long extracellular N-terminus (which contains a short disulfide bonded cys-cys Loop), four transmembrane spanning domains (TM_1-TM_4), and a short extracellular C-terminus. Two intracellular Loops connect TM_1-TM_2 and TM_3-TM_4 while an extracellular loop connects TM_2-TM_3. The N-terminus contains the ligand

recognition site for 5-HT (Eisele et al 1993) and TM_2 lines the channel pore. The intracellular loop connecting TM_3-TM_4 contains amphipathic α helix, named as the MA stretch or HA stretches and presents multiple consensus sequences for phosphorylation by various kinases (reviewed in Peters et al., 2005).

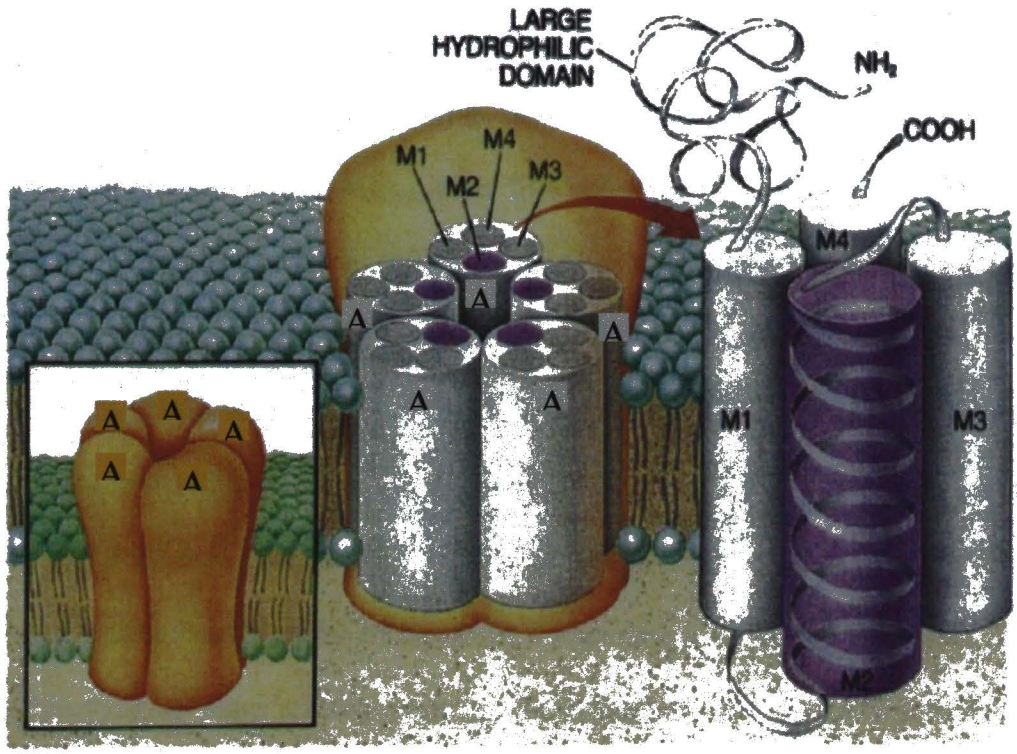

Figure 1 Overall Structure of $5HT_{3A}$ receptor. The receptor has five subunits, each subunit consists of large extracellular N-terminus, four transmembrane domains and short extracellular C-terminus.

Alignment of TM_2 domain from A subunit with that of the other members of the ligand-gated ion channel superfamily reveals many similarities (Karlin and Akabas 1995), particularly with regard to the rings of negative charges that are localized at the

extracellular and intracellular borders of TM_2 and the hydrophobic residue located at position two of the channel (Thompson and Lummis, 2003). Furthermore studies with substituted cysteine accessibility method have demonstrated the largely helical structures of TM_2 (Reeves et al., 2001), which is similar to the other members of the superfamily.

5-HT_3 receptor assembly occurs in the endoplasmic reticulum (ER), and receptors are expressed on the plasma membrane of the cell. The human homomeric receptor (5-HT_{3A}) has three potential N-linked glycosylation sites at positions N-104, 170 and 186. The human heteromeric receptor (5-$HT_{3A/B}$) has five potential glycosylation sites at positions N-47, 91, 133, 163 and 198. N-linked glycosylation is required for receptor stability (Boyd et al., 2002). Another study indicated that there are four N-glycosylation sites in homomeric (5- HT_{3A}) receptors at N 5, 81, 147 and 163. When these four asparagine residues were mutated individually in the human 5-HT_{3A} receptor, three mutant receptors (81, 147 and 163) lost their binding affinity to a significant extent and these receptors were found predominantly in the intracellular compartment. These observations indicate that N-glycosylation plays an important role in expression of receptor and formation of ligand binding site (Monk et al., 2004). A similar study was carried out in murine 5-HT_{3A} receptor, in which the presence of three N-glycosylation sites at positions N-104, 174 and 190 were reported. In this study N109 was found to play a role in receptor assembly, while 174 and 190 were required for plasma membrane targeting and ligand-binding (Quirk et al., 2004). Together, all these observations emphasize that N-glycosylation is required for normal function of 5-HT_3 receptors. However N-glycosylation is not the only requirement for receptor trafficking. Other residues also have a role in that process.

Price and co-workers reported that in the extracellular N-terminal domain of mouse 5-HT_3 receptor, Tyrosine 50 plays an important role in receptor trafficking to the cell surface and Tyrosine 91 plays an important role in receptor assembly (Price and Lummis, 2004). In a similar study carried on murine 5-HT_3 receptor, it was reported that Glutamate 235 plays a role in receptor trafficking (Schreiter et al., 2003).

C. 5-HT_3 Receptor Subtypes, Homomeric vs. Heteromeric Receptors

To date five subunits of the 5-HT_3 receptor has been cloned. The genes for subunits A and B of 5-HT_3 receptors are located in close proximity on chromosome 11. The genes for subunits C, D and E are clustered on chromosome 3q27 (Niesler et al., 2003). Subunit A has been cloned from numerous mammalian species (Belelli et al., 1995;Miyake et al., 1995; Lankiewicz et al., 1998). Subunit B has been identified in human and rodent tissues (Davies et al., 1999; Dubin et al., 1999; Hanna et al., 2000). An alternatively spliced variant of subunit A has been identified in receptor cDNA of mouse (Hope et al., 1993), rat (Miquel et al., 1995) guinea pig and ferret (Lankiewcz et al., 1998). The subunits C, D and E have been cloned only from human tissues. The subunits A, B and C have been reported to be present in most of the body tissues of the adult humans, for example brain, colon, intestine, lungs, muscles and stomach. The subunit D is expressed only in kidney, liver and intestine, and subunit E is expressed only in colon and intestine. The D subunit is unlike the other 5-HT_3 receptor subunits in that it lacks a signal peptide in N-terminus, suggesting that the N-terminus is intracellular. In

addition the N-terminus is truncated relative to the other 5-HT_3 receptor subunits and only contains the part of ligand binding domains. Therefore the D subunit may not form a functional ion channel (Niesler et al., 2003).

The A subunits form functional homomeric receptors which retain the full pharmacology and most of the functional characteristics of the 5-HT_3 receptor endogenously expressed in neuronal preparations (Yakel et al., 1988; Lambert et al., 1989; Kawa et al., 1994). The B subunits can only form heteromeric receptors, as they cannot assemble to form ligand-binding domains (Barrera et al., 2005) and cannot exit the endoplasmic reticulum in the absence of subunit A (Boyd et al., 2003). No functional studies have been published to date on any heteromeric 5-HT_3 receptors containing subunits C, D or E. In the case of homomeric 5-HT_3 receptors, all the five subunits are of type A while in the case of heteromeric 5-HT_3 receptors, three subunits are B and two subunits are A arranged as B-B-A-B-A (Barrera et al., 2005).

The heteromeric receptor (5-$HT_{3A/B}$) displays reduced Ca^{2+} permeability, altered current voltage rectification and high single channel conductance relative to the homomeric receptor (Davies et al., 1999; Dubin et al., 1999; Das et al 2003). The homomeric and heteromeric 5-HT_3 receptors also differ from each other in terms of pharmacological properties (Brady et al., 2001; Hapfelmeier et al., 2003). The heteromeric 5-HT_3 receptors show markedly less sensitivity towards allosteric modulators such as n-chain alcohols and volatile anesthetics (Stevens et al., 2005), ethanol and tricholoroethanol (Hayrapetyan et al., 2005) and channel blockers such as

Picrotoxin (Das and Dillon 2003). Also, there is a slight difference in curare sensitivity of homomeric and heteromeric 5-HT_3 receptors (Davies et al., 1999).

D. The ligand binding domains of the 5-HT_3 receptor

There are two ligand-binding sites present in each 5-HT_3 receptor (Gehlert et al., 1991). These ligand-binding sites are located alternatively at the interface of N-terminal domains of two adjacent subunits. The subunit interface is formed from two different faces of two different subunits. These faces are known as principal face and complementary face.

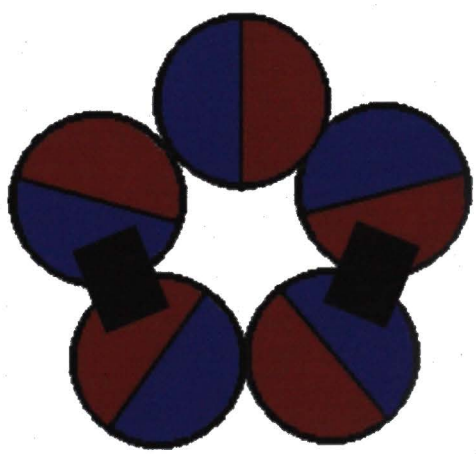

Figure 2 Position of ligand binding sites in the homomeric 5-HT_3 receptors. Each receptor has two ligand binding sites located alternately on the subunit interface. The subunit interface is formed of principal face (red) of one subunit and complementary face (blue) from another subunit.

Six smaller groups of amino acid residues have been identified in the N-terminal domain of the 5-HT_3 receptors. These groups are named Loop A, B, C, D, E and F (Sine et al., 2002). Similar loops have been reported to be present in other family members such as nACh receptors and $GABA_A$ receptors. In three-dimensional structure Loop A, B and C form the principal face, while Loops D; E and F form the complementary face.

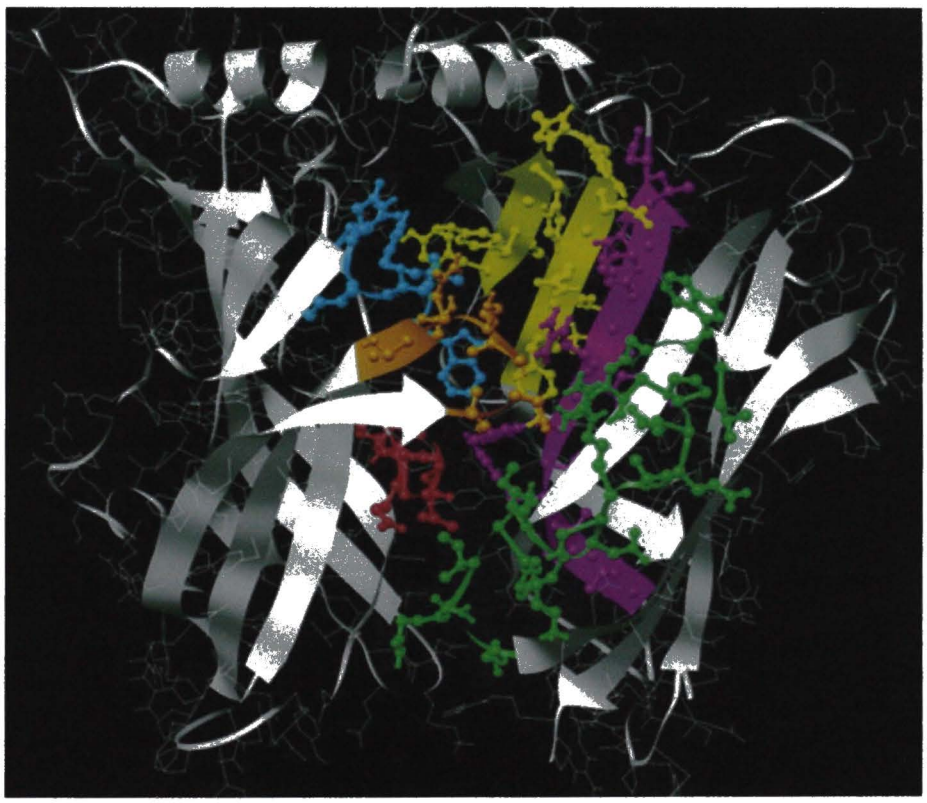

Figure 3 Molecular model for the ligand-binding site of 5-HT_{3A} receptor. Left side represents principal face with loop A (red), B (sky blue) and C (orange). Right side represents complementary face with loop D (magenta), E (yellow) and F (green), (Yan and White, 2005).

In 1993, Eisele and co-workers confirmed the location of the ligand-binding site to be the extracellular N-terminus. They constructed a chimeric receptor in which the N-terminal domain from the α7 neuronal nACh receptor subunit was linked to C-terminal receptor portion of the 5-HT_{3A} receptor subunit. This chimeric receptor possesses the nACh receptor pharmacological properties and the 5-HT_3 receptor channel properties (Eisele et al., 1993). Tryptophan residues present in Loop A, B and D of the nACh receptor was identified as putative ligand binding residues through photoaffinity labeling (reviewed in Galzi and Changeux, 1995). Corresponding tryptophans in the mouse 5-HT_3 receptors W 90 (Loop D), W 121 (Loop A) and W 183 (Loop B) as well as all the other tryptophan residues present in N-terminus (W 60, 95, 102, 195 and 214) were mutated to serine and tyrosine (Spier and Lummis 2000). Mutations at W 90, 183 and 195 had marked effects on the ligand binding and receptor function, suggesting a critical role in ligand recognition. In another study, Beene et al. (2002) indicated that W 183 was the cation-π binding site that interacts with the quaternary ammonium group of ACh. Mutations at W 90, R 92 and Y 94 (Loop D) had differential effects on affinity of 5-HT and other 5-HT_3 receptor ligand suggesting that these ligands have different points of contact with the receptor (Yan et al., 1999). Together all these observations suggest that Loop A, B and D which are known to play a critical role in the process of ligand-binding in nACh receptor also play a major role in ligand-binding process of 5-HT_{3A} receptors.

The recent discovery of the crystal structure of the Acetylcholine Binding Protein (ACHBP), a protein homologous to the extracellular domain of the nACh receptor, has provided the generalized three-dimensional configurations of the ligand binding domains

of the members of the cys loop family (Brejc et al., 2001). The ACHBP is a soluble protein found in the snail *Lymnae stagnalis*. It has a homopentameric structure, which resembles the extracellular N-terminal domain of the members of the ion channel superfamily but lacks the transmembrane domains present in the receptors. It binds the neurotransmitter acetylcholine, and terminates its actions. It can be used as an experimental model for ligand-gated ion channels as it contains most of the conserved residues including the residues involved in ligand binding, similar to the members of the superfamily (Brejc et al., 2001). The structure of the extracellular domain of α 7 the nACh receptor has 23% protein sequence identity with the ACHBP and that of the 5-HT_3 receptor has 19% protein sequence identity with the ACHBP (Price and Lummis 2004). Based on this homology, two homology models of the extracellular N-terminal domain of 5-HT_3 receptors were constructed by two different groups.

In the first homology model, Reeves and co-workers (Reeves et. al., 2003) explained the binding pocket with a focus on contact points for 5-HT. In this model, the N-terminal domain of 5-HT_3 receptor was divided among five loops namely A, B, C, D and E. The sixth loop, i.e. Loop F, is not described in this model since the three dimensional aspects of loop F were not fully understood in ACHBP at that time. However, the researchers suggested the role of Loop F amino acid residues in the process of ligand binding. In this model, 76% of the residues that were identified to be within $5A^0$ of 5-HT are conserved and are located in loops A to E. Loop C is the only region, which contains several non-conserved residues, underscoring the possible role of these

amino acid residues in differential sensitivity of agonists and antagonists across species of 5-HT_{3A} receptors.

There are three residues that may form hydrogen bonds with 5-HT, and thus are involved in correct localization of agonist and in coupling the ligand-binding phenomenon with gating. These three hydrogen-bond forming residues are serine (S) 182, glutamate (E) 236 and arginine (N) 128. The hydrogen bond is formed from the backbone of serine, and from the functional groups of glutamate and arginine. These hydrogen bonds favor the tight binding of 5-HT and lower the energy barrier for channel opening.

The indole group from 5-HT binds in the hydrophobic pocket formed by Y and W residues, and is thought to form a cation $-\pi$ interaction with W 183 (Beene et al., 2001). The OH group of 5-HT is modeled as being in a pocket formed by R 92, D229 and Q 151. The ring systems of 5-HT are in between Y234 and W183 (Reeves et. al., 2003).

In the second homology model, Maksay and co-workers (Maksay et al., 2003) explained the binding of antagonists such as granisetron, tropisetron, ondansetron, dolasetron and curare. They compared N-terminal domains of the 5-HT_{3A} receptors from three different species, mouse, human and guinea pig. They used as an underlying assumption that a similarity exists between the structures of the extracellular N-terminal domains 5-HT_{3A} receptor and the nACh receptor. Thus, in this model the extracellular N-terminal domain of the 5-HT_{3A} receptor is divided into six loops, namely A, B, C, D, E and F. According to them, the amino acid residues present in Loop C form a characteristic protrusion that harbors the ligand-binding cavity of $9A^0$. A similar

protrusion was reported from electron microscopic studies of nACh receptors (Unwin et al., 2002). The aromatic residues tryptophan (W90, W183) and tyrosine (Y143, 153 and 234) are present in the narrow back portion of the binding cavity with isoleucine (I) 230 in the back wall. A hydrophilic acidic environment is created in the binding cavity near the surface of receptor by the presence of four acidic residues E129, D204, E/D229 and E236 to attract the basic ligand. The tryptophan residue present at 183rd position forms a threshold between the hydrophilic and hydrophobic areas of the binding site. The models for human and mouse 5-HT_{3A} receptors were found to be structurally similar but had slightly different interface interactions along the binding site. There is a huge difference between curare potency of mouse and human 5-HT_{3A} receptors. This difference was attributed to the non-conserved residues present in Loop C and to a lesser extent in Loop A-F. In mouse 5-HT_{3A} receptor, a hydrogen bond may be formed between a hydroxyl group at 7' position (7'-OH) and carboxylic group from aspartate present at 229th position (D229), and serine at 227th position (S227). Similarly, a hydrogen bond can also form between a hydroxyl group at 12' position (12'-OH) and glutamate present at 129th position (E129) and the leucine present at 238th position (K238). In the case of the human 5-HT_{3A} receptor, the long distance between the carboxylic group of glutamate residue at 229th position (E229) and the hydroxyl group present at 7' position in curare (7'-OH) does not allow formation of any hydrogen bond between them. According to the authors, this presence of hydrogen bond in mouse 5-HT_{3A} receptor may play a significant role in conferring its high curare potency. In case of the human 5-HT_{3A} receptor, the curare moves deeper in the binding cavity. This may be due to the less steric hindrance offered

by serine present at 230th as compared to the isoleucine present in mouse 5-HT_{3A} receptor (Maksay et al., 2003).

Both these models were based on the experimental finding that the tryptophan residue present at 183rd position forms a cation-π interaction with serotonin (Beene et al., 2002).

Mouse **Human**

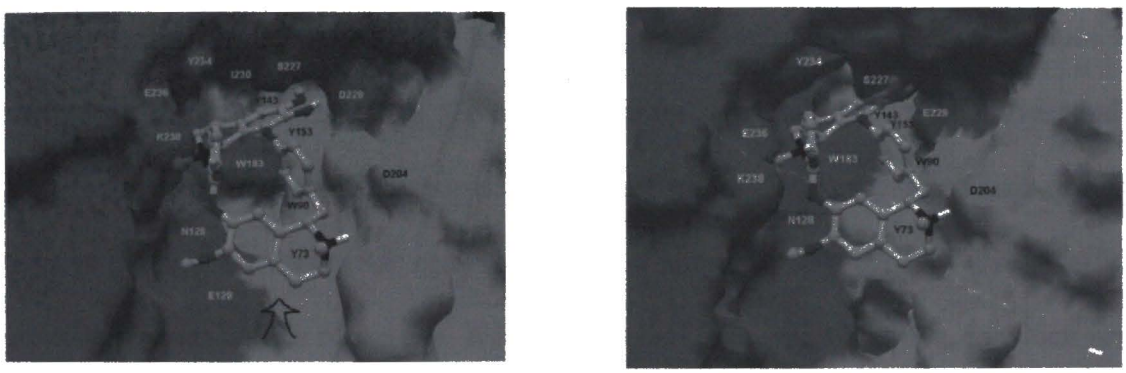

Figure 4 Homology Model of Ligand binding site of 5-HT_{3A} receptor. The dark gray area represents + (principal) face and the light gray area represents – (complementary) face. The arrow represents entry of curare molecule in the binding pocket (Maksay et al, 2003).

E. Interspecies studies

It has long been known that the 5-HT_{3A} receptors from different mammalian species have differential affinities for antagonists such as Curare (curare) and partial agonists such as 2-methyl serotonin and *m*-chlorophenyl biguanide (*m*CPBG) (reviewed in Peters et al., 1999). Several investigators constructed interspecies chimera and point mutant receptors to identify domains that are responsible for alterations in responsiveness to drugs (Lankiewicz et al., 1998; Hope et al., 1999; Mochizuki et al., 1999). From these studies, the domains implicated in ligand recognition include amino acid residues that correspond to Loop C region of the nACh receptor. Alignments of the corresponding Loop C domains in the 5-HT_3 receptors from mouse, rat, guinea pig and human reveal seven to eight differences. Rat receptors have an approximately 13 fold greater affinity for *m*CPBG than human receptors. A human-rat 5-HT_3 receptor chimera, in which seven amino acid residues present in Loop C region of the human receptor were substituted with that of the rat orthologs, had the same *m*CPBG sensitivity as that of rat receptor (Mochiziki et al., 1999).

Along with the interspecies differences for the ligand affinities, the 5-HT_3 receptor shows differences in the binding locations for different ligands. Mutations at W 90, R92 and Y94 (Loop D) had differential effects on affinity of 5-HT and other ligands of the 5-HT_3 receptor, which suggests that these ligands have different points of contact with the receptor (Yan et al., 1999). In another study it was found that two structurally different agonists, i.e., 5-HT and *m*CPBG, interact with different amino acid residues present in the binding site of mouse 5-HT_{3A} receptor. Four amino acid residues present

in Loop C region were found to be important in the process of ligand recognition; these residues were F226, Y234, D229 and I228. Among these four residues I228 and D229 were found to be specifically interacting with 5-HT, while F226 and Y234 were found to be interacting with both i.e. 5-HT and *m*CPBG (Schulte et al., 2005).

The competitive antagonist curare is an excellent tool to identify regions of the N-terminal domain of the mouse and human 5-HT_{3A} receptor responsible for ligand-binding. Wild-type mouse and human 5-HT_{3A} receptors are 84% identical at amino acid level yet there is an approximately 1800-fold difference in their curare potencies. The curare IC_{50} for wild type human receptor has been found to be 2550 nM while curare IC_{50} for wild type mouse receptor has been reported to be 1.4 nM (Hope et al., 1993; Belleli et al., 1995). Thus this huge difference in the potency is likely due to the non-conserved amino acid residues present in the binding site of mouse and human 5-HT_{3A} receptors. Curare is a competitive antagonist for muscle type nicotinic acetylcholine and 5-HT_3 receptors (Yan et al., 1998). It is a plant-derived alkaloid used for centuries by South Americans to prepare poison arrows for hunting wild animals. It causes respiratory paralysis and subsequent asphyxiation, which ultimately results in death (Sobell et al., 1972). It is used as a muscle relaxant in balanced anesthesia. Figure 2 shows the structure of *d*-Tubocurarine.

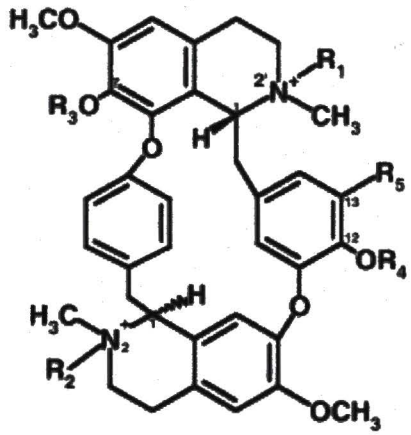

R_1	R_2	R_3	R_4	R_5	Stereo Isomer 1	1'	NAME
CH_3	H	H	H	H	S	R	*d*-Tubocurarine
H	H	H	H	H	S	R	Tubocurine

Figure 5 Structure of *d*-Tubocurarine (Yan et al., 2002)

In our laboratory, a previous student examined the contribution of Loops C and F in conferring the differential curare potency of the human and mouse 5-HT_{3A} receptors. ('Molecular determinants of at recombinant 5-Hydroxytryptamine$_3$ receptor' Master's thesis by Xiaofei Wen). Two chimeric receptor cDNAs were constructed from mouse and human in which the distal 1/3 part of the N-terminus was substituted with that of the receptor cDNAs of other species. The chimeric mouse 5-HT_{3A} receptor in which the distal 1/3 portion of the N-terminus was substituted with corresponding human orthologs, mimicked the curare potency of human wild-type 5-HT_{3A} receptor. While the human chimeric receptor in which the distal 1/3 part of the N-terminus was substituted with corresponding mouse orthologs had curare potency similar to that of the mouse wild-type 5-HT_{3A} receptor (Fig 6). Together these results suggest that the distal 1/3 portion of the N-terminal domain of the 5-HT_3 receptors is sufficient for determining the curare

potency. There are sixteen total non-conserved amino acid residues present in the distal 1/3 region of the wild type mouse and human 5-HT_{3A} receptors. Out of these sixteen residues, seven are present in Loop C, six are present in Loop F and three are present outside Loop C and Loop F.

A previous student from our laboratory had constructed a chimeric receptor on the human background, in which the entire Loop C region was substituted by corresponding mouse orthologs (Hch Loop C receptor). This receptor has a curare IC_{50} of 41 nM, which is closer to the curare IC_{50} of 12.19 nM for the wild-type mouse receptor compared to the curare IC_{50} of 1.81 μM for the wild-type human receptor (Fig. 6). However, when seven point mutant receptors were constructed on human background in each of which one amino acid was mutated to corresponding mouse orthologs, none of them could mimic the curare potency of Hch Loop C receptor (Fig. 7). This observation suggests that an interaction of two or more than two amino acid residues is required to confer curare potency of the receptor. A chimeric receptor was constructed on human background in which four amino acid residues were mutated to corresponding mouse orthologs (H-2/3 Loop C receptor). These four mutations were Y217Q, M223I, E224D and Y228S. This receptor has a curare IC_{50} of 34 nM, which indicates that all the non conserved amino acid residues present in Loop C region are not necessary for conferring curare potency of Hch Loop C receptor ('Molecular determinants of d-Tubocurarine binding at recombinant 5-Hydroxytryptamine$_3$ receptor' Master's thesis by Xiaofei Wen).

The homology model suggests that amino acid residues present in Loop C play a major role in the process of ligand binding (Reeves et al., 2003, Maksay et al., 2003).

Other researchers also reported the importance of amino acid residues present in Loop C, in the process of ligand binding. It has been reported that a number of residues from Loop C are responsible for conferring the potency of the receptor for agonist m-CPBG (Mochizuki et al., 1999), and competitive antagonist curare (Yan et al., 1999). It has been shown with the chimeric receptor on the mouse background that, I228, D229 and I230 have a significant effect on the curare potency of the receptor (Hope et al., 1999).

F. Gating

The binding of agonist at the ligand-binding site of the receptor results in a series of conformational changes in the receptor, which ultimately cause the opening of the ion channel. This phenomenon is called 'gating'. The process of gating is not well understood in any of the receptors belonging to the superfamily of ligand-gated ion channels. However some recent studies offer explanation for certain steps in the gating phenomenon.

The first study was carried out on the $GABA_A$ receptor, which focuses on the later steps in the gating process (Kash et al., 2003). Investigators of this study aligned the molecular sequence of various α subunits of $GABA_A$ receptor with that of ACHBP. The aligned sequences showed that several acidic residues are highly conserved in Loops 2 and 7 regions of the $GABA_A$ receptor while two basic residues are conserved in the linker region between TM_2 and TM_3 that faces the extracellular environment (2-3L). Based on their experimental findings in this study, the investigators proposed that, each of the two acidic residues present in loop 2 and 7 (D149 and D57) are in close proximity with one of

the two basic residues present in 2-3L region (K279). This proximity gives rise to an electrostatic interaction between these oppositely charged amino acids. Mutagenesis studies performed on D57, D149 and K279 suggest that when ligand (GABA) binds at the ligand binding site of the receptor, the conformation of the receptor changes and as a result the position of loop 7 and 2-3L region gets rearranged, triggering the opening of the channel. Mutagenesis of D57, D149 to K or A and mutagenesis of K279 to D decreased potency of GABA in patch-clamp electrophysiological studies. Charge reversal (D57K, K279D) and (D149K, K279D) restored GABA potency. In the double mutant receptor (D57C, K279C) a disulphide bond formed in the presence of an oxidizing reagent, regardless of whether GABA was present. In contrast, in double mutant receptor (D149C, K279C), a disulphide bond formed only in the presence of GABA. These results suggest that the electrostatic interaction between D149 (loop 7) and K279 plays an important role in channel opening (Kash et al., 2003).

In another study, Bouzat and co-workers tried to explain the details of the gating phenomenon using a chimeric receptor in which the extracellular N-terminus of the 5-HT_{3A} receptor was replaced with ACHBP binding domain. This receptor was found to be present on the cell membranes of the mammalian cells; however, it wasn't a functional receptor because of the incompatibility at the interface due to inter-domain coupling. So a functional homology model of this receptor was constructed using *Torpedo* acetylcholine receptor. This homology model suggested a physical proximity between the three interconnecting loops from the binding domains of extracellular N-terminus and the loop connecting transmembrane domain two and three. It was found that the three

interconnecting loops including loops 2 and 7 of the binding domain together alter the binding affinity of the receptor, which reflects enhanced function. These three interconnecting loops along with the M_2-M_3 linker loops transfer the conformational changes started with binding of agonist to the binding site with the ion pore as well as couple the functional state of the pore with the binding site. In the overall scheme, it can be said that as a result of agonist binding, a twisting motion is generated in the binding pocket, which travels along to reach the pore lining M_2 domain to allow flow of cations. The structural compatibility between the four inter-domain loops is a general requirement for this allosteric coupling in the ion channels (Bouzet et al., 2004). It was suggested that in the initial steps of the gating process, the agonist-induced displacement of two tyrosine residues (Y 143 and 153) is present in the aromatic binding pocket of the extracellular domain. This displacement forms new hydrogen bonds, which along with the other structural rearrangements initiates gating process in mouse 5-HT_{3A} receptor (reviewed in Peters et al., 2005). In a later study Reeves and co-workers showed that K81 in loop 2 of the 5-$HT_{3A/B}$ receptor interacts with the M_2-M_3 linker to cause opening. This is non-electrostatic interaction as no positively charged residues are present (Reeves et al., 2005).

A recent study carried out by Lummis and co-workers explains the role of a conserved proline residue present at the apex of the loop connecting TM_2 and TM_3 domains of the cation selective members of the superfamily (5-HT_3 receptor and nACh receptor). According to this study, the conserved proline residue (pro8*) acts like a hinge to facilitate movement of the channel-lining TM_2 domain. The replacement of proline

with C, V, A, N, K or G resulted in non-functional receptors, with no change in receptor trafficking or ligand-binding properties. This indicates that the proline residue is involved in gating process. Using unnatural amino acid mutagenesis, a series of proline analogs were created, which gave rise to three types of mutant receptors, i.e., non-functional receptors, intermediately functioning receptors and receptors showing no significant change in function as compared to wild type receptors. The proline analogs strongly favoring 'trans' conformation gave rise to the receptors that failed to respond to the agonist but were expressed on the cell membrane. Among the intermediately functional and wild type like receptors, those having proline analogs favoring 'cis' isoform were found to be highly sensitive to ligand. Thus the investigators found a strong link between the conformation of the residue present at 8* position and gating of the 5-HT_3 receptor. Based on their experimental findings, the researchers proposed a hypothesis to explain the gating phenomenon in 5-HT_3 receptor. The hypothesis states that when the ion channel is closed, the proline 8* residue is in the 'trans' conformation. Ligand binding causes proline 8* residue to change its conformation to 'cis' form, which results in reorientation of the M_2 domain to open the channel (Lummis et al., 2005).

G. Gaps in our knowledge

A well-defined model of the precise spatial configuration of the ligand-binding site is lacking for any of the nACh receptor superfamily members. The definition of amino acid residues comprising the ligand binding is critical for a better understanding of the gating process. The 5-HT_3 receptor is a good model system to study the agonist

recognition site. The availability of homomeric 5-HT_3 receptor (5-HT_{3A} receptor), along with the differences in the affinities and efficacies of the agonists and competitive antagonists, makes this receptor convenient for chimeric receptor analysis.

The model of the ligand-binding site of the 5-HT_{3A} receptor has been reported based on its sequence homology with the ACHBP (Brjec et al., 2001). However, details about the amino acid residues involved in the process of ligand binding and their individual roles in that process have to be determined experimentally. The electrophysiological recordings with curare will be helpful in determining the roles of amino acid residues and their interactive effects on binding and/or gating process. Experimental evidence shows that amino acid residues present in Loop C play a critical role in forming binding site for curare (Hope et al., 1999). D229 is one of the two acidic residues present in Loop C of the mouse 5-HT_3 receptor, which is present in the close proximity of the ligand or may interact with the ligand (Tairi et al., 2003). However, specific details of the interactions of the amino acids present in Loop C and Loop F are not fully understood yet.

H. Hypothesis

The previous student from Dr. Machu's laboratory has demonstrated that the wild-type mouse $5HT_{3A}$ receptor has a curare IC_{50} of 13 nM, and the wild-type human $5HT_{3A}$ receptor has a curare IC_{50} of 1800 nM. Through the use of mouse-human and human-mouse chimeric receptors, she identified the distal one-third of the N-terminus as

being critical for determining curare potency. Within the distal one-third of the N-terminus are Loops C and F.

A human chimeric receptor containing Loop F mouse orthologs, has the curare IC_{50} is 132 nM. Two mutations within Loop F are reported to be sufficient to obtain the IC_{50} of 132 nM. A human chimeric receptor containing Loop C orthologs has a curare IC_{50} of 41 nM. None of the seven mutant human receptors containing single mouse receptor orthologs has an IC_{50} of 41 nM. However, a human chimeric receptor containing four mouse receptor orthologs (H-Y217Q, M223I, E224D, Y228S) has a curare IC_{50} of 34 nM (Zhang and Machu, 2005). Loop C residues in 5-HT3A receptors interact to confer curare potency.

Based on these previous findings, we hypothesize that some minimum number of mutations are required in Loop C for curare potency, one of which is E224D.

Specific Aim # 1: No point mutant human $5HT_{3A}$ receptor containing mouse orthologs in Loop C has the curare sensitivity (IC_{50} = 41 nM) of the human Loop C chimeric receptor containing all seven-mouse orthologs. A four point mutant receptor including E224D mutation has an IC_{50} of 34 nM, which is not significantly different from the IC_{50} of 41 nM. The goal is to determine which combination of residues is required for curare potency of Loop C, with emphasis on E224D.

Specific Aim # 2: The two point mutant receptors, which displayed the greatest enhancement in curare potency relative to human wild-type receptor, are H-V237I and H-R219K. The goal is to determine the effect of their interaction on the curare IC_{50} of Hch-Loop C receptor.

II. MATERIAL AND METHODS

A. Reagents

d-Tubocurarine (curare), 5-Hydroxytryptamine (serotonin/5-HT), Ampicillin sodium salt, pyruvic acid sodium salt, collagenase, phenol: chloroform (5:1), phenol: chloroform: isoamyl alcohol (25:24:1), cesium chloride (CsCl) and Luria-Bertani medium (LB) were purchased from Sigma Chemical Co. (St. Louis MO). Agarose was obtained from Bio-Rad Laboratories (Hercules, CA). All the restriction endonucleases, T4 DNA ligase, and their buffers were purchased from New England Biolabs, Inc (Beverly, MA). The primers were synthesized by Midland Certified Reagent, Inc. Midland TX and MWG Biotech, Inc. (High Point, NC). Nuclease free water and mMESSAGE mMACHINE T3 and T7 transcription kits were obtained from Ambion Inc. (Austin, TX.). Wizard *plus* SV Minipreps DNA purification System was from Promega Corporation (Madison, WI). Transformer Site Directed Mutagenesis kit was purchased from Amersham Pharmacia Biotech, Inc. (Piscataway, NJ). QuikChange Site-Directed mutagenesis Kit was purchased from Stratagene (La Jolla, CA). Amersham Pharmacia Biotech, Inc provided competent E.coli MutS cells; The Epicurian Coli XL-Blue supercompetent cells were obtained from Stratagene (La Jolla, CA). Stock solutions of 5-HT (1mM) and d-Tubocurarine (1mM or 10μM) were prepared in Modified Barth's solution (MBS) and were frozen. Aliquots were thawed each day and diluted to desired concentrations. Sterile water for irrigation (Baxter Healthcare Corporation, Deerfield, IL) was used to prepare all solutions. Akira Miyake, Yamanouchi Pharmaceutical Co.,

provided Tsukuba, Japan human wild type 5-HT3A receptor cDNA. David Julius, University of California at San Francisco, CA, provided Mouse wild type 5-HT_{3A} receptor cDNA. Ewen Kirkness, Institute of Genomic Research Rockville, MD, provided Mouse and human 5-HT_{3B} receptor cDNAs.

B. Construction of Chimeric 5-HT_{3A} Receptors

Chimeric receptors were prepared from human and mouse wild type 5-HT_{3A} receptor cDNAs. Sequential alignment of distal one-third part of N-terminal domains of mouse and human 5-HT_{3A} receptors are shown in Figure 5.

```
                Signal Peptide
Mou  1   MRLC I PQVLLALFLSMLTAPGEGSRRRATQARDTTQPALLRLSDHL
Hum  1   MLLWVQQALLALLLPTL LAQ GEARRSR..........NTTRPALLRLSDYL

                                                   Loop D
Mou 47   LANYKKGVRPVRDWRKPTTVSIDVIMYAILNVDEKNQVLTTYIWYR
Hum 42   LTNYRKGVRP VRDWRKPTTVSIDVIVYAILNVDEKNQVLTTYIWYR

         Loop D                          Loop A
Mou 93   QYWTDEFLQWTPEDFDNVTKLSIPTDSIWVPDILINEFVDVGKSPN
Hum 88   QYWTDEFLQWNPEDFDNI TKLSIPTDSIWVPDILINEFVDVGKSPN

             Loop E                                  Loop B
Mou 139  IPYVYVHHRGEVQ NYKPLQ LVTACSLDIYNFPFDVQN CSLTFTSWL
Hum 134  IPYVY I RHQGEVQ NYKPLQVVTACSLDIYNFPFDVQN CSLTFTSWL

         Loop B                Loop E                Loop C
Mou 185  HTIQDINITLWRSPEEV RSDKSI F I NQGEWELLEVFP QFKEFSI D IS
Hum 180  HTIQDINISLWRLPEKVKSDRSVFMNQGEWELLGVLP YFREFSMESS

                Loop C
Mou 232  NSY AEMKFYVI IRRR
Hum 227  NYYAEMKFYVVIRRR
```

Figure 6 The human chimeric 5-HT_{3A} receptor cDNAs used in the present study were generated by substitution of nucleotides encoding non-conserved residues in Loop C with that of mouse receptor cDNA.

All the human Loop C chimeric receptor cDNAs used for this project were prepared in this laboratory. Some of them were constructed prior to the start of this thesis project. The chimeric receptors that I used for my project are:

H-Y217Q/R219K/M223I/Y228S/V237I

H-Y217Q/R219K/M223I/S225I/Y228S

H-M223I/E224D

H-R219K/V237I

H-Y217Q/Y228S

H-M223I/E224D/Y228S

H-Y217Q/M223I/E224D

The human 5-HT_{3A} receptor cDNA was subcloned into PCR Script™ AMPSk (+) vector at the *Srf I* site in the polylinker. The chimeric receptors were constructed by QuikChange Site-Directed Mutagenesis method (by thermal cycling) and Transformer Site-Directed Mutagenesis method.

C. Site Directed Mutagenesis

Sequences of primers used in Mutagenesis:

All the primers used in the experiments are listed in Table 1. The 'Mutation' column indicates the sequence number of amino acid whose codon has been mutated. The nucleotide encoding the amino acid on each number's left side was mutated to the one on the right side. For each QuikChange mutagenesis reaction, two primers were constructed, both of which contain the same mutations and are complementary. In the transformer mutagenesis reaction, one primer introduced the mutation of interest and second primer deleted a unique restriction site in the polylinker.

Mutant Receptor	**cDNA Template**	**Mutation Introduced**	**Primers**
H-Y217Q, Y228S (QuikChange)	H-Y228S	Y217Q	**5' ->3' direction:** **GAA CTC CCG AAA CTG GGG CAG CAC CCC CAG C** **3' -> 5' direction:** **C GAC CCC CAC GAC GGG GTC AAA GCC CTC AAG**

H-M223I, E224D, Y228S **(QuikChange)**	H-M223I, E224D	Y228S	**5' ->3' direction:** **GAA CTT CAT TTC TGC ATA GGA GTT ACT GCT GTC GAT GCT G** **3' -> 5' direction:** **G TCG TAG CTG TCG TCA TTG AGG ATA CGT CTT TAC TTC AAG**
H-Y217Q, M223I, E224D **(QuikChange)**	H-M223I, E224D	Y217Q	**5' -> 3 direction:** **GCT GAA TTC CCG AAA CTG GGG CAG CAC CCC CAG C** **3' ->5' direction:** **C GAC CCC CAC GAC GGG GTC AAA GCC CTT AAG TCG**
H-Y217Q, R219K, M223I, S225I, Y228S **(Transformer)**	H-Y217Q, R219K, M223I, Y228S	S225I	**3' ->5' direction:** **GTC AAA TTC CTT AAG TCG TAT CTT TAG TCA TTG AGG**
H-M223I, E224D **(Transformer)**	HWT_A	M223I, E224D	**3' ->5' direction:** **G AAA GCC CTT AAG TCG TAG CTG TCG TCA TTG**

H-Y217Q, R219KM223I, Y228S, V237I (Transformer)	H-Y217Q, R219K, M223I, Y228S	V237I	**3' ->5' direction: CCG CCG GCG GAT GAT TAC GTA GAA CTT CAT TTC TGC**
H-R219K/V237I (Transformer)	H-R219K	V237I	**3' ->5' direction: CCG CCG GCG GAT GAT TAC GTA GAA CTT CAT TTC TGC**

Table 1 Primers used for construction of chimeric receptors by Site-Directed Mutagenesis.

Site Directed Mutagenesis by Thermal Cycling.

A) Mutant strand synthesis reaction: In this step, the oligonuclotide primers each complementary to the two strands of cDNA are extended during thermal cycling by PfuTurbo DNA polymerase. Incorporation of the oligonuclotide primers generated a mutated plasmid containing staggered nicks. For this reaction, two double stranded primers were diluted to 63ng/µl, and 2µl of each primer were used. The (dam^+) dsDNA template was diluted to 50ng/µl. Both the primers were placed in PCR microcentrifuge tubes along with 5 µl of 10 x reaction buffers, and 1µl of dNTP mixture. Nuclease free water was added to make a total volume of 50 µl. To this mixture 1µl of *PfuTurbo* DNA polymerase (2.5U/µl) was added. The mixture was then placed in the thermal cycler for sixteen cycles. The cycling parameters are listed in Table 2.

Segment	Temperature	Time
1	95^0C	30 Seconds
2	95^0C	30 Seconds
3	55^0C	1 Minute
4	68^0C	1 Minute/kb of plasmid length.

Table 2 Cycling parameters for the QuikChange Site-Directed Mutagenesis method.

B) Dpn I Digestion of the Amplification products: Dpn I endonuclease is specific for methylated and hemimethylated DNA and is used to digest parental DNA template and to select for mutation-containing synthesized DNA. For this step, 1µl of Dpn I restriction enzyme was added to each amplification reaction and incubated for one hour in a 37^0C heat block.

C) Transformation of XL 1-Blue Supercompetent cells: In this step, the reaction mixture containing the mutant cDNA strands was transformed into Supercompetent XL 1-Blue cells. Cells were gently thawed on ice. For each transformation reaction, 50µl was transferred to a prechilled 15ml BD Falcon polypropylene round bottom tube. The mixture was swirled gently and incubated for 30 minutes on ice. The mixture was then placed in a 42^0C bath for 45 seconds for 'heat pulsing' and then immediately placed on ice for two minutes. Five hundred µl of LB medium, preheated at 42^0C, was added to the reaction mixture. The mixture was incubated for one hour at 37^0C with shaking at 225-250 rpm. After one hour, 250µl of the reaction mixture was transferred to LB-Ampicillin agar plates. The plates were incubated overnight at 37^0C.

D) Identification of mutant cDNAs: Five colonies were picked from the LB-Ampicillin agar plates, and each colony was incubated in a mixture of 3 ml LB and Ampicillin (0.1μg/ml) at 37^0C with shaking at 225-250 rpm for 12 hours.

DNA Miniprep: The bacterial cultures were centrifuged at room temperature for 5 minutes. The supernatant liquid was discarded, and the cell pellet was thoroughly resuspended with 250 μl of Cell Resuspension solution. To the resuspended pellet, 250 μl of Cell Lysis solution was added, followed by 10 μl of Alkaline Protease. The mixture was incubated for 5 minutes at room temperature. Finally, 350 μl of Neutralization Solution was added and the mixture was centrifuged at top speed for 10 minutes at room temperature. The clear lysate was transferred into a column and the column was attached to a vacuum adapter. The column was then washed with 1 ml of Column Wash Solution, transferred to another collection tube, and centrifuged at top speed for 4 minutes at room temperature. The column was then transferred to a sterile 1.5 ml microcentrifuge tube, incubated with 60 μl of RNase free water for 2 minutes at room temperature and centrifuged at top speed for 1 minute at room temperature.

The cDNA obtained was used for final transformation. Minipreps were performed on the culture from each colony. The concentration of each purified cDNA was measured spectrophotometrically. Presence of desired mutation was identified by dideoxynucleotide sequencing of cDNA. Two hundred and fifty μl of cells from each tube was combined with 250μl of sterile glycerol and kept in -20^0C as stocks to be used in large-scale cDNA preparation.

Plasmid cDNA sequencing: The plasmid cDNA was sequenced at the Core Facility in the Biotechnology Institute of Texas Tech University, Lubbock, TX. The sequences were analyzed with Bio Edit software.

Site Directed Mutagenesis by USE mutagenesis protocol:

A) Primer Phosphorylation: The primers were combined with 10X T_4 polynucleotide kinase (T_4 PK) Buffer (500 mM NaCl, 100 mM Tris-HCl, 100 mM $MgCl_2$, 10 mM dithiothreitol), 3 µl of 10 mM ATP and 2 µl T_4 PK (5-10 units) in a 1.5 ml microcentrifuge tube. The final volume was adjusted to 30 µl with sterile water. The reaction mixture was incubated for 30 minutes at 37^0C followed by heating at 65^0C for 10 minutes. The phosphorylated primers were stored at -20^0C (For the following steps, these phosphorylated primers were used).

B) Denaturation of Plasmid DNA and Annealing of Primers to the DNA template: In a sterile 1.5 ml microcentrifuge tube, 100 ng of plasmid cDNA (Human wild-type 5-HT_{3A}-PCRScript) was mixed with 100 ng of selection primer, 100 ng of mutagenic primer and 10X annealing buffer (2 µl). The final volume was adjusted to 20 µl with sterile water. The reaction mixture was incubated for 3 minutes at 100^0C, and immediately placed on ice for 5 minutes.

C) Synthesis of mutant cDNA strands: In a sterile 1.5 ml microcentrifuge tube, 10X reaction buffer (3 µl), T_4 DNA Polymerase (1 µl), T_4 DNA Ligase (1 µl) and Sterile water

(5 μl) were mixed thoroughly and incubated for two hours at 37^0C, followed by heating at 70^0C for five minutes.

D) Primary selection by Restriction Digestion: The reaction mixture from the previous step was mixed with the appropriate restriction enzyme (2 μl), suitable buffer (5 μl) and when required BSA (5 μl). The final volume was adjusted to 50 μl with sterile water. The reaction mixture was incubated for two hours at a temperature suitable for the enzyme used followed by heating at 70^0C for five minutes.

E) First Transformation: Competent *E. coli Mut S* cells were gently thawed on ice. For each transformation reaction, 200μl was transferred to prechilled 15ml Falcon tube. To each aliquot, 40 μl of digested cDNA from the previous reaction was added. The mixture was swirled gently and incubated for 30 minutes on ice. The mixture was incubated in a 42^0C bath for 45 seconds for 'heat pulsing' and then immediately placed on ice for two minutes. One ml of LB medium, preheated at 42^0C was added to the reaction mixture, and the mixture was incubated for two hours at 37^0C with shaking at 225-250 rpm. After two hours, 4 ml of LB and 5μl of Ampicillin were added and the mixture was incubated overnight at 37^0C with shaking at 225-250 rpm.

F) DNA Miniprep: The Miniprep procedure was carried out as described on the previous page.

G) Final Transformation: The final transformation was performed following the transformation protocol using Competent *E. coli* XL1 blue cells.

F) DNA Miniprep: The Miniprep procedure was carried out as described on the previous page.

D. Cesium Chloride Gradient Purification of cDNA

A) Preparation of Bacterial Culture (Lysis by Alkali): Bacteria were incubated in a mixture of two liters of LB and Ampicillin (0.1μg/ml) at 37^0C, with shaking at 225-250 rpm for 16-20 hours. The culture was transferred to large Beckman centrifuge tubes and centrifuged at 8000 rpm at 15 minutes. The LB broth was discarded and the pellets were resuspended in 40 ml of solution I (50 mM glucose, 25 mM Tris, 10 mM EDTA pH (8.0). Four ml of lysozyme solution (10 mg/ml) was added to the resuspended solution, followed by 80 ml of freshly prepared solution II (0.2N NaOH, 10 % SDS). The contents were mixed thoroughly and stored at room temperature for 5 minutes. Sixty ml of ice-cold solution III (3M Potassium acetate, glacial acetic acid) was added, and the contents were mixed thoroughly by shaking several times. The mixture was stored on ice for 10 minutes. At the end, a flocculent white precipitate was formed. The mixture was centrifuged at 8000 rpm at 4^0C for 20 minutes. The supernatant was filtered through 4 Kim Wipes, and 0.6 volumes of isopropanol were added to it. The mixture was stored at room temperature for 10 minutes. The mixture was then transferred to 50 ml sterile centrifuge tubes and centrifuged at top speed in a table top centrifuge for 10 minutes. The supernatant was discarded and the pellet was washed with 70% ethanol in water. Dry pellets were stored at -20^0C.

B) Cesium Chloride Gradient Purification of DNA: The pellets obtained from alkaline lysis were resuspended in 8 ml TE buffer, pH 7.4 in a sterile Falcon tube. Cesium Chloride (8.8 gm) was dissolved in the resuspended liquid, and 0.8 ml of ethidium bromide (10 mg/ml) was added. The mixture was centrifuged in a table top centrifuge for 5 minutes. The proteins precipitated during centrifugation were discarded and the supernatant liquid was transferred to Beckman quick seal tubes (5/8 in x 3 in) via a 5 cc syringe with 18-gauge needle. The remaining volume of the tube was filled to the tube neck with 'Filler solution' (0.85 mg/ml of CsCl in TE buffer). The Beckman tubes were sealed using metal sealing caps. The tubes were centrifuged for 24 hours in an ultracentrifuge at 65800 RPM in a Ti 80 rotor at 22^0C. The cDNAs were removed from the tube with 5cc syringes with 18 gauge needles. The cDNAs were introduced to new Beckman tubes, and the tubes were filled with Filler solution, sealed and subjected to ultracentrifugation for 24 hours. The cDNAs obtained were transferred to disposable 15 ml Falcon tubes and extracted with isoamyl alcohol to remove ethidium bromide. Three volumes of water were added to the extracted cDNAs. Two volumes of ethanol were added to the mixture. The DNA was then allowed to precipitate for 30 minutes, and the precipitates formed were removed by centrifugation at top speed for 10 minutes in the table top centrifuge. The precipitate was then washed two times with 70% ethanol in water, dried and resuspended in nuclease free water. The concentration was determined with a UV spectrophotometer.

E. *In Vitro* transcription

A) **Preparation of cDNA:** Twenty micrograms of wild type and mutant receptor cDNAs were linearized with Bam H I, Xho I or Hind III for four hours in a heat block at 37^0C. The restriction enzyme used in the reaction was then digested with proteinase K by incubating the reaction mixture at 37^0C for 30-45 minutes. The cDNA was then extracted with 1:1 volume of phenol chloroform: isoamyl alcohol (25:24:1). The possible remnants of phenol were removed by extracting three times with chloroform in 1:1 volume. The cDNA was then precipitated with 5M ammonium acetate (RNase free) solution (0.1x total volume) and two volumes of 100% ethanol. The mixture was kept in the freezer (-20^0C) for 30 minutes to allow the precipitation to take place. The precipitate was then centrifuged at full speed for 10 min at room temperature and then washed three times with 500 μl of 70% ethanol in RNase free water. The precipitate was then allowed to dry in a speed vacuum at 30^0C for 20 minutes. Finally, the precipitate was resuspended in 20 μl of RNase free water, and the concentration of DNA was measured with a spectrophotometer.

B) **Preparation of cRNA:** For the *in vitro* transcription reaction, 1.2μg of linearized cDNA was used from the previous step. To it were added 10μl of ribonucleotide mixture (2X) (15mM ATP, CTP, UTP and 3mM GTP), 2μl of reaction buffer (10X), 2μl of enzyme Mix (T3 RNA polymerase, RNAse inhibitor) and DEPC water to make a total volume of 20μl. The mixture was incubated for 1 hour in a heat block at 37^0C. The next step was digestion of original DNA template present in the mixture. The mixture was incubated

with 1μl of RNAse FREE DNAse I for fifteen minutes at 37^0C. After 15 minutes, 15μl of 5M ammonium acetate and 115 μl of water were added to stop the reaction. The cRNA was purified by extracting with phenol: chloroform (5:1) Phenol was removed from the cRNA by extracting three times with chloroform in 1:1 proportion. One volume of isopropyl alcohol was added and the mixture was kept in -20^0C for 30 minutes. The cRNA concentration was measured with a spectrophotometer. To avoid any contamination during handling, the cRNA was aliquot 25μl per microcentrifuge tube, and these tubes were stored at -80^0C.

F. Preparation and maintenance of *Xenopus* oocytes

Oocytes were obtained from *Xenopus laevis*, a frog species native to South Africa. The mature oocytes (stage V-VI) have a diameter of 1-1.2 mm. (Dumont et al., 1978), and they are visible without a microscope.

Frogs were anesthetized by immersion in ice cold 0.12% 3-amino benzoic acid ethyl ester for 20 min. After removal through a small incision in the frog's abdomen, ovarian lobes were placed in modified Barth's solution (MBS) containing in (mM) NaCl 88, KCl 1, $NaHCO_3$ 2.4, HEPES 10, $MgSO_4$ 0.82, $Ca(NO_3)_2$ 0.33, and $CaCl_2$ 0.91 (pH 7.5). Ovarian lobes were manually dissected into clumps of 4-10 oocytes and then subjected to chemical separation and defolliculation. Clumps of oocytes were placed in the medium containing 2 mg/ml Collagenase Type 2 and in (mM) NaCl 83, KCl 2,

$MgCl_2$ 1, and HEPES 10 (pH 7.5) and gently rocked for 2 hours. This step was repeated one more time using new media and new collagenase solution. Lastly, oocytes were washed with MBS and stored in incubation media composed of ND 96, containing (in mM) NaCl 96, KCl 2, $CaCl_2$ 1.8, $MgCl_2$ 1 and HEPES 5 (pH 7.5), plus 10mg/l streptomycin, 50mg/l gentamycin, 10000-units/l penicillin, 96mg/l sulfamethoxazole, 19mg/l trimethoprim, 0.5mM theophylline, and 2mM sodium pyruvate.

G. Microinjection of *Xenopus* oocytes with receptor cRNA

Aliquots of cRNA were centrifuged at 15000x g, and the ethanol removed with a tuberculin syringe. After air-drying, the pellet was resuspended in a volume of RNase free water to yield the desired concentration of cRNA/50-100nl. The cRNA was drawn up in a micropipette (10-20 μM tip size). In a volume of 50-100 nl, cRNA was injected into the animal/vegal pole equator of each Oocyte. Oocytes were stored in incubation medium in Corning cell well plates at room temperature and incubation medium was changed daily. Oocytes were recorded from 24 hours/7 days following injection.

H. Electrophysiological recordings of the 5-HT_{3A} Receptor Responses

Oocytes were perfused in 100 μl volume chamber with MBS via a roller pump, 2 ml/minute (Cole-Parmer Instrument, Co., Chicago, IL). Two glass electrodes (1.2mm outside diameter and 1-10 megaohm resistance) filled with 3M KCL were used to impale oocytes. A Warner instrument model OC-725B or OC-725C Oocyte clamp (Hamden, CT) was used to voltage clamp oocytes at -70mV. Clamping currents were plotted on a

strip chart recorder (Cole-Parmer Instrument, Co., Chicago, IL). Serotonin in the absence and presence of curare was applied for 30 seconds every five minutes. Peak current amplitudes were calculated.

To obtain a 5-HT concentration response curve with each receptor construct, suitable concentrations of 5-HT were prepared using a 1mM stock solution. Twenty five μM 5-HT was used to obtain baseline currents. The inward currents were recorded for 5-HT concentrations from 0.1 to 25 μM. Serotonin mediated currents were expressed as percentage of the 25 μM 5-HT currents.

For curare concentration response curves, a concentration of 5-HT that gives approximately 10% of the maximal response (EC_{10}) was used as a baseline. Suitable curare concentrations were prepared using 1mM and 10 μM curare stock solutions, and dissolving them in the baseline 5-HT solution. The baseline 5-HT solution was applied in absence and presence of curare. Data were expressed as a percent inhibition of the control, baseline response.

I. Data Analysis

Graphpad Prism (San Diego, CA) was used to calculate EC_{50}s, IC_{50s} and Hill coefficients. One-way ANOVAs and students paired t-tests were performed with Instat software.

The values in the 5-HT concentration response curves data were expressed as a percent change from the baseline response. The baseline responses were obtained by

averaging the 5-HT mediated response before and after the response to 5-HT, or 5-HT plus curare. For curare inhibition response curves, percent inhibition was calculated by subtracting the current obtained from curare + 5-HT from the average current obtained with 5-HT alone; the difference was divided by the average 5-HT mediated current, and the quotient was multiplied by100. The curare IC_{50} values for wild-type mouse and human receptors and human chimeric receptors were compared by One-Way Analysis of Variance (ANOVA) and Tukey-Kramer post-hoc analysis.

III. RESULTS

To determine the roles of amino acid residues in Loop C of the $5HT_{3A}$ receptor and their interactive effects on binding and/or gating processes, we tested seven chimeric receptors on the human receptor background for their curare potency. We also tested the curare sensitivities of heteromeric mouse and human wild-type receptors ($5HT_{3A/B}$ receptors). This will serve as a basis for future work to investigate the roles of Loop C and F in the process of ligand recognition in heteromeric receptors.

Previous research in our laboratory has shown that a human chimeric receptor, in which the entire Loop C is substituted by corresponding mouse orthologs (Hch Loop C receptor), has a curare IC_{50} of 40.77±1.9 nM (Hill coefficient = 1.3±0.08) (Figure 6). This chimeric receptor has seven mutations on the human receptor background. The Hch Loop C's curare potency is less than that of the mouse wild-type receptor (IC_{50} = 12.19±0.47 nM). Two other chimeric receptors were constructed on the human receptor background. In the first receptor (H-217->228 receptor), six out of the seven Loop C amino acid residues were mutated to corresponding mouse orthologs (V237I mutation was excluded). The curare IC_{50} of this receptor was found to be 40.27±2.5 nM (Hill coefficient = 1.1±0.09). In the second receptor, four out seven amino acid residues were mutated to corresponding mouse orthologs (H-2/3 Loop C receptor/Hch Loop C minichimeric receptor). The curare IC_{50} of this receptor was found to be 34.35±2.58 nM (Hill coefficient = 1.0±0.09). Comparison of IC_{50} values of wild-type and the four, six,

and seven point mutant receptors was significant (one-way ANOVA, $F_{(3,16)}= 40.8$; $p < 0.0001$). Tukey-Kramer post-hoc analysis revealed that the IC_{50} values for all three chimeras were significantly greater than that of the mouse wild-type receptor ($p < 0.001$). However, none of the chimeric receptors' IC_{50} values were different from each other ($p > 0.05$), (Figure 6). From these observations, it is evident that an interaction between two or more of the mouse orthologs is required to confer the curare potency of Loop C region. Among these seven point mutant receptors tested by a previous student, the receptor with highest curare potency was H-V237I, which has the curare IC_{50} of 0.35 μM (Hill coefficient = 1.0±0.07). While the receptor with least curare potency was H-E224D, which has a curare IC_{50} of 8.9±0.51 μM (Hill coefficient = 1.2±0.08) (Figure 7). The E224D mutation, on human receptor background produced a rightward shift in the curare potency, however the H-2/3 Loop C receptor, which contains E224D mutation, has a high curare potency of 34.35±2.58 nM (Hill coefficient = 1.0±0.09). This suggests that the interaction of aspartate residue with the other three mutated residues present in H-2/3 Loop C receptor has a positive effect on the curare potency of the receptor.

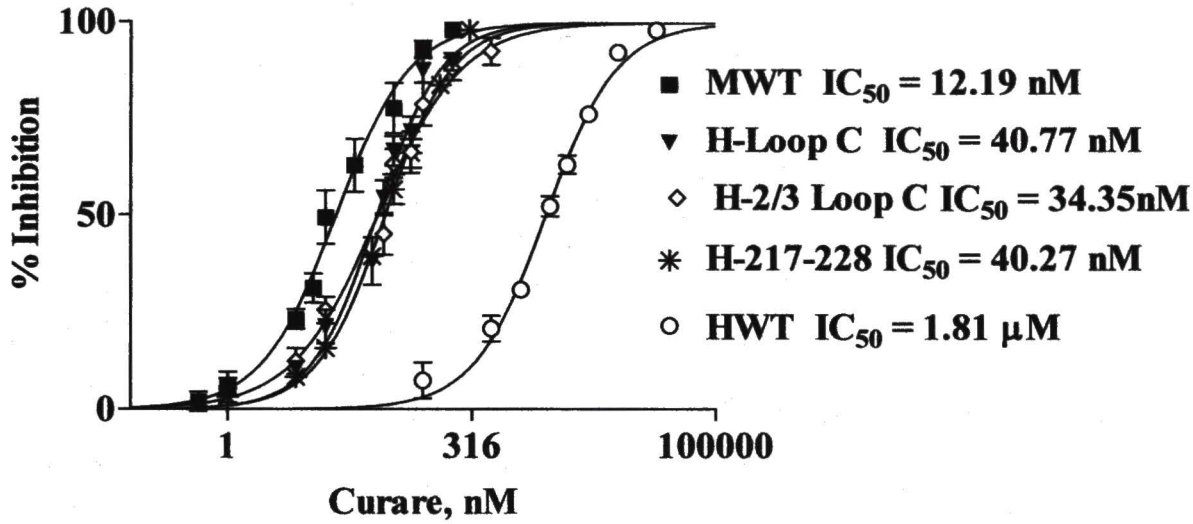

Figure 7 A human chimera containing six of seven mutations in Loop C (V237 was not mutated), Hch-217->228, and H-2/3 Loop C (217,223,224,228) had the same curare potency as Hch-Loop C.

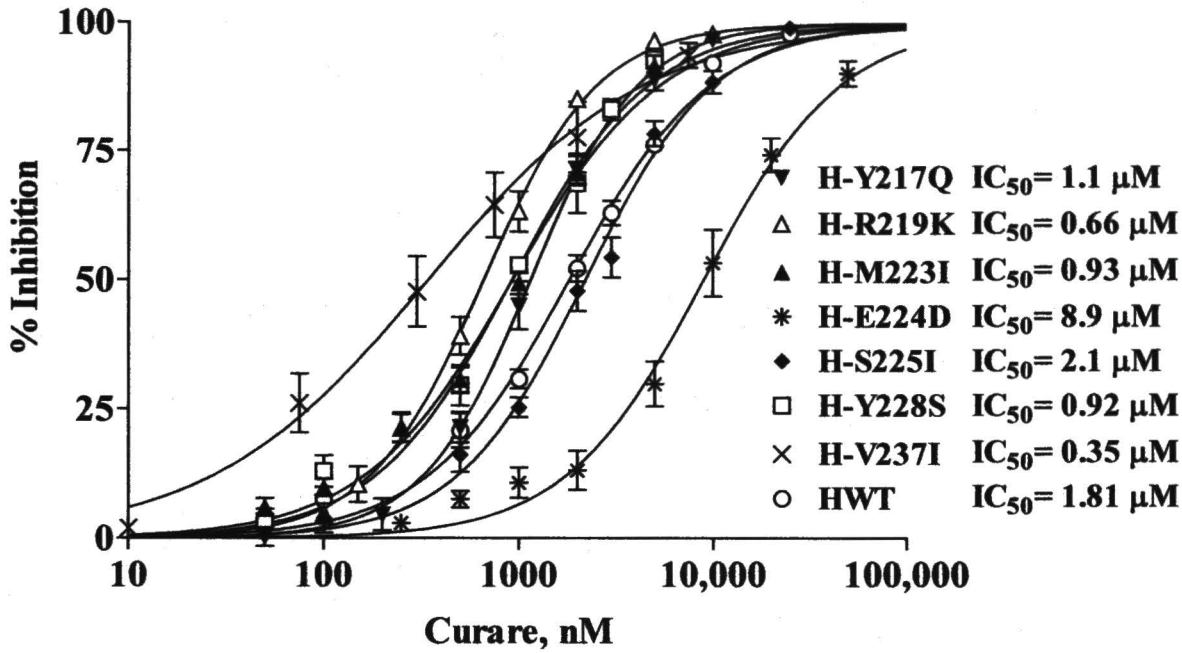

Figure 8 Curare concentration response curves were performed in human 5-HT_{3A} receptors containing point mutant mouse orthologs in Loop C. None of the point mutant receptors reduced the curare IC_{50} to that of the human Loop C chimeric receptor (Hch Loop C receptor).

A. Characterization of 5-HT response curves in human chimeric 5-HT_{3A} receptors and heteromeric human and mouse 5-$HT_{3A/B}$ receptors

For the characterization of mutant and wild type receptors, a two-electrode voltage clamp electrophysiological recording system was used. Inhibition of 5-HT mediated currents by curare was determined in wild type and chimeric receptors. Initially, 5-HT response curves were generated for all the receptors, with 25 μM 5-HT as the

baseline concentration. Responses to a range of 5-HT concentrations (0.1- 20 μM 5-HT) were recorded to generate 5-HT concentration response curves. For each receptor, we experimentally determined the concentration of 5-HT generating 5-15% of the maximum response (EC_{10}), to provide a uniform basis for comparing curare potencies. In each receptor, an EC_{10} of 5-HT was used in the generation of curare inhibition response curves.

For the curare inhibition response curves, the baseline 5-HT concentration was applied in the absence and presence of curare. The percent inhibition of the baseline response obtained by each curare concentration was calculated. The curare concentration, at which 50% inhibition of the baseline response obtained, was reported as the curare IC_{50}.

Mutant Receptor	**EC_{50} (μM)**	**Hill Coefficient**
H-Y217Q, Y228S	2.1 ± 0.18	1.8 ± 0.26
H-M223I, E224D, Y228S	6.3 ± 0.70	1.9 ± 0.36
H-Y217Q, M223I, E224D	1.6 ± 0.08	2.0 ± 0.20
H-Y217Q, R219K, M223I, S225I, Y228S	0.9 ± 0.09	1.7 ± 0.36
H-M223I, E224D	2.3 ± 0.13	2.0 ± 0.21
H-Y217Q, R219K, M223I, Y228S, V237I	0.8 ± 0.06	3.1 ± 0.85
H-R219K, V237I	1.6 ± 0.07	1.9 ± 0.14
HWT_{A+B}	6.8 ± 0.33	2.0 ± 0.53

MWT_{A+B}	2.0 ± 0.15	1.4 ± 0.16

Table 3 Summary of the 5-HT concentration response curves showing EC_{50s} and Hill Coefficients for wild type and chimeric 5-HT_3 receptors.

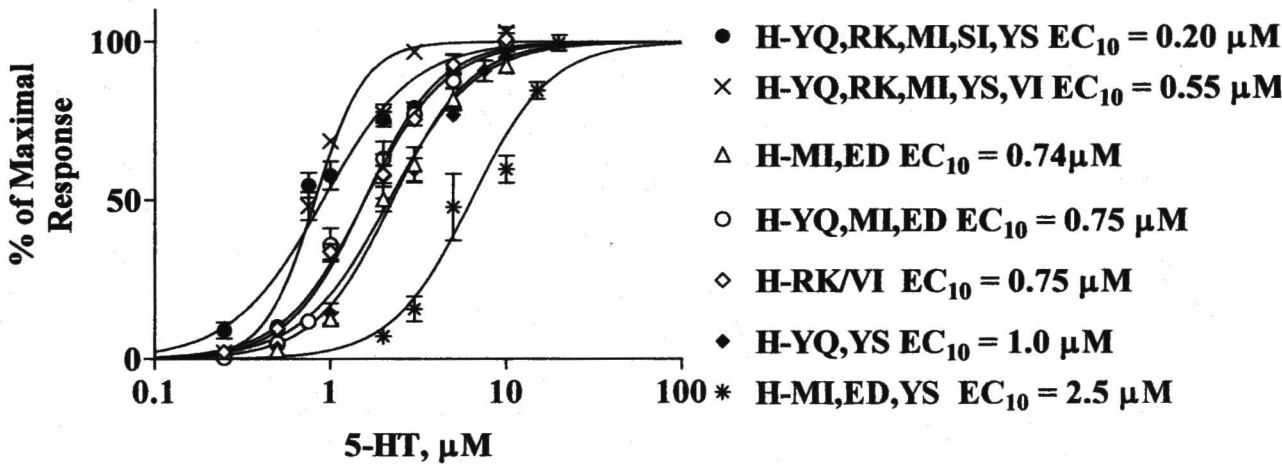

Figure 9 Serotonin response curves for chimeric $5HT_{3A}$ receptors on human background.

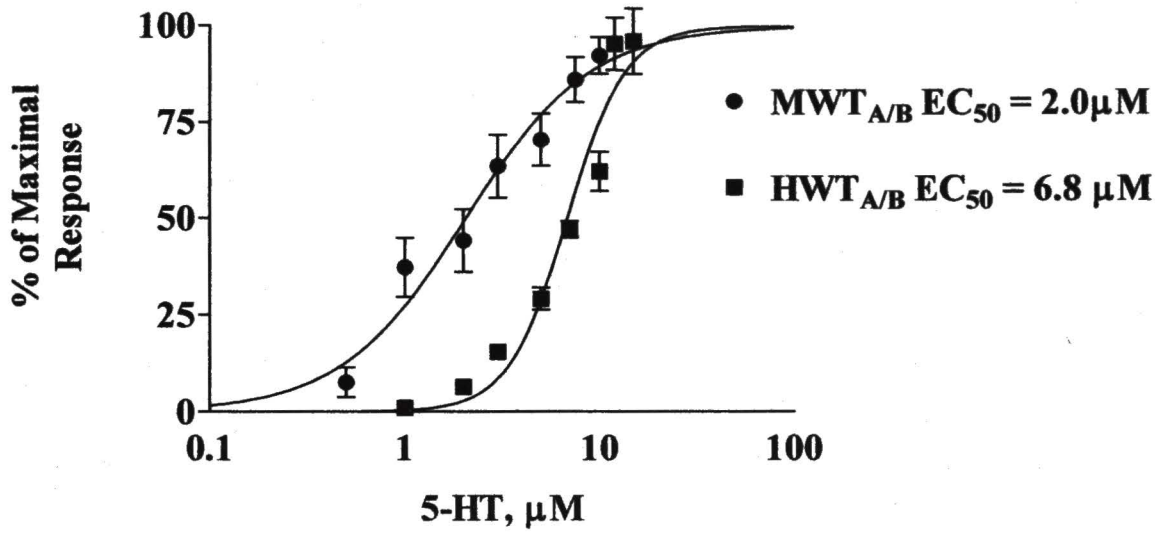

Figure 10 Serotonin response curves for the wild type mouse and human heteromeric receptors ($5HT_{3A/B}$ receptors).

B. Curare potencies of chimeric human 5-HT_3 receptors

1. E224D mutation in the H-2/3 Loop C receptor is essential for generating the curare IC_{50} of 34 nM.

It has been shown that the D229E mutation has the greatest effect on curare potency in mouse $5HT_{3A}$ receptor although the curare potency was only reduced to ten fold as compared to the mouse wild type receptor (Hope et al., 1999). The point mutation studies conducted in our laboratory showed that H-E224D receptor has a curare IC_{50} of 8.9 μM (Hill coefficient = 1.2±0.08) (Figure 7). This suggests a possibility that an

interaction of aspartate residue with other mouse residues present in H-2/3 Loop C receptor is required to produce a curare IC_{50} of 34.35 nM (Hill coefficient = 1.0±0.09).

To test this hypothesis, we constructed a human chimeric receptor (H-Y217Q, R219K, M223I, S225I, Y228S) containing five mouse orthologs in Loop C but without E224D mutation. The curare inhibition response curve for this receptor is shown in Fig 10. The curare IC_{50} for this receptor was found to be 102±8.2 nM (Hill coefficient = 0.9±0.08). The previously tested receptor, Hch-217->228 containing six of the seven Loop C mutations (Figure 6), has a curare IC_{50} of 40.27±2.5 nM (Hill coefficient = 1.1±0.09). These two observations suggest that the E224D mutation plays an important role in conferring curare potency of Hch Loop C receptor.

We next examined the role of S225I mutation in conferring curare potency in H-Y217Q, R219K, M223I, S225I, Y228S receptor. There was no significant difference in the curare potency of H-Y217Q, R219K, M223I, S225I, Y228S (curare IC_{50} = 102±8.2 nM, Hill coefficient = 0.9±0.08) as compared to the curare potency of a previously tested receptor H-Y217Q, R219K, M223I, Y228S (curare IC_{50} = 101±3.10 nM Hill coefficient = 1.4±0.05) (Figure 10). This suggests that S225I mutation does not play a significant role in conferring curare potency of Hch Loop C receptor.

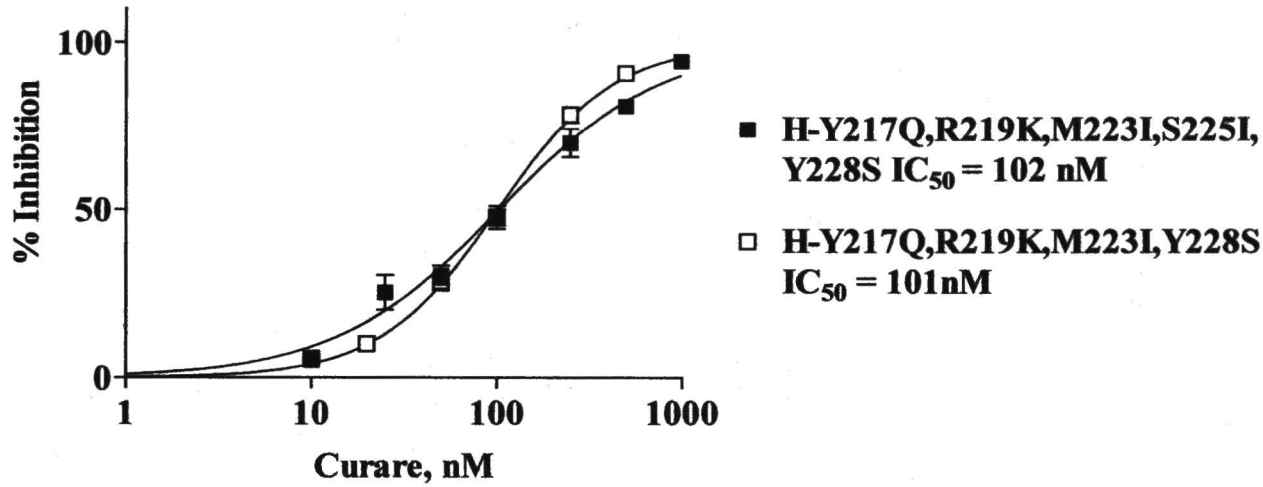

Figure 11 Curare inhibition response curves for H-Y217Q, R219K, M223I, Y228S and H-Y217Q, R219K, M223I, S225I, Y228S. No significant difference was found in the curare IC_{50}S of these two receptors (student's t-test, p=0.90).

2. All four mutations present in 2/3 Loop C receptor are essential.

The chimeric receptor H-2/3 Loop C (H- Y217Q, M223I, E224D, Y228S) has a curare IC_{50} of 34.35±2.58 nM (Hill coefficient = 1.0±0.09). This gives rise to a critical question of whether all four of these mutations are required to produce a curare IC_{50} of 34.35 nM. To answer this question we constructed four chimeric receptors, two of them containing three mutations on human background (H-M223I, E224D, Y228S and H-Y217Q, M223I, E224D), and two of them containing two mutations on human background (H-Y217Q, Y228S and H-M223I, E224D) (Figure 11). Thus, including a previously tested receptor H-Y217Q, M223I, Y228S, some of the possible combinations

of the four mutations present in H-2/3 Loop C receptor were tested for their curare potencies.

The curare IC_{50} of H-Y217Q, M223I, E224D was found to be 456.2±28.9 nM (Hill coefficient = 1.1±0.06). The curare IC_{50} of H-M223I, E224D, Y228S was found to be 121.3±7.1 nM (Hill coefficient = 1.3±0.10). The curare IC_{50} of H-Y217Q, M223I, Y228S was found to be 175±7.8 nM. The curare IC_{50} of H-M223I, E224D receptor was found to be 1388±68.8 nM (Hill coefficient = 1.1±0.04) and the curare IC_{50} of H-Y217Q, Y228S receptor was found to be 353.4±23.0 nM (Hill coefficient =1.3±0.10). Thus all of these receptors show lower curare potencies as compared to H-2/3 Loop C receptor. Since none of the receptors containing two or three mutations of H-2/3 Loop C receptor could mimic its curare potency, it is evident that all the four mutations present in H-2/3 Loop C receptor are essential to produce a curare IC_{50} of 34 nM. One-way ANOVA revealed a significant difference across curare IC_{50} values in the chimeric receptors, $F_{(5,26)} = 220$, $p < 0.001$. All two and three point mutant receptors' IC_{50} values were less than that of H-2/3 Loop C, $p < 0.001$, except for H-M223I, E224D, Y228S, and $p < 0.05$, Tukey-Kramer's post-hoc test.

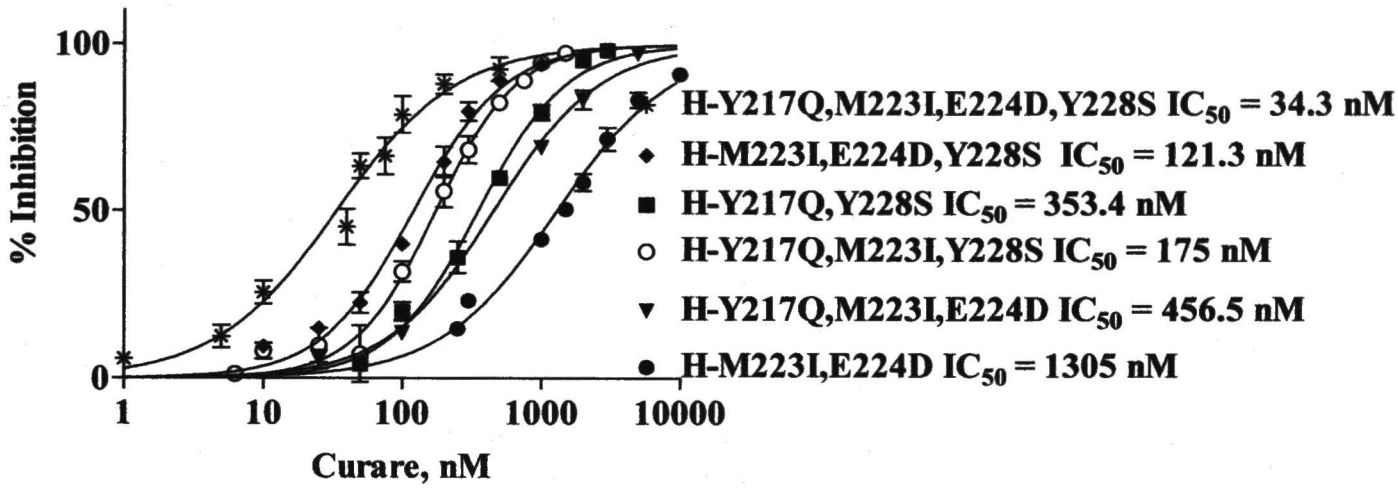

Figure 12 Curare inhibition response curves for chimeric receptors on human background, each of which contains a different permutation of two or three mutations from H-2/3 Loop C receptor. None of these receptors could mimic the curare potency of H-2/3 Loop C receptor.

3. The interaction of R219K and V237I do not enhance the curare potency.

Among the seven point mutant receptors on human background tested for their curare potency, the two receptors with the greatest increase in curare potency were H-R219K (curare IC_{50} = 660 nM, Hill coefficient = 1.5±0.04) and H-V237I (curare IC_{50} =350 nM, Hill coefficient = 1.0±0.07). To test the effect of their interactions in conferring Loop C curare potency, we constructed two chimeric receptors on the human background containing these mutations.

The first chimeric receptor was H-Y217Q, R219K, M223I, Y228S, V237I. Since the V237I mutation enhanced the curare potency to the highest extent among the seven point mutant receptors (figure 7), it was added to H-Y217Q, R219K, M223I, Y228S receptor (Figure 12). The goal was to determine whether V237I mutation would reduce the curare potency below 100 nM. Instead, the curare IC_{50} of H-Y217Q, R219K, M223I, Y228S, V237I receptor was found to be 152.5±7.31 nM (Hill coefficient = 1.6±0.10), suggesting that V237I mutation does not compensate for the absence of the E224D mutation. The curare IC_{50} for this chimeric receptor was not significantly different than that of the H-Y217Q, M223I, Y228S receptor (Student's t test, $p = 0.06$).

The curare IC_{50} of H-R219K, V237I receptor was found to be 875.9±46.34 nM (Hill coefficient = 1.4±0.12) suggesting that the interaction of R219K and V237I do not show any additive or synergistic effects. The observation that the combination of these two mutations reduced the curare potency further underscores the observation that interactions of key Loop C mouse orthologs confer curare potency.

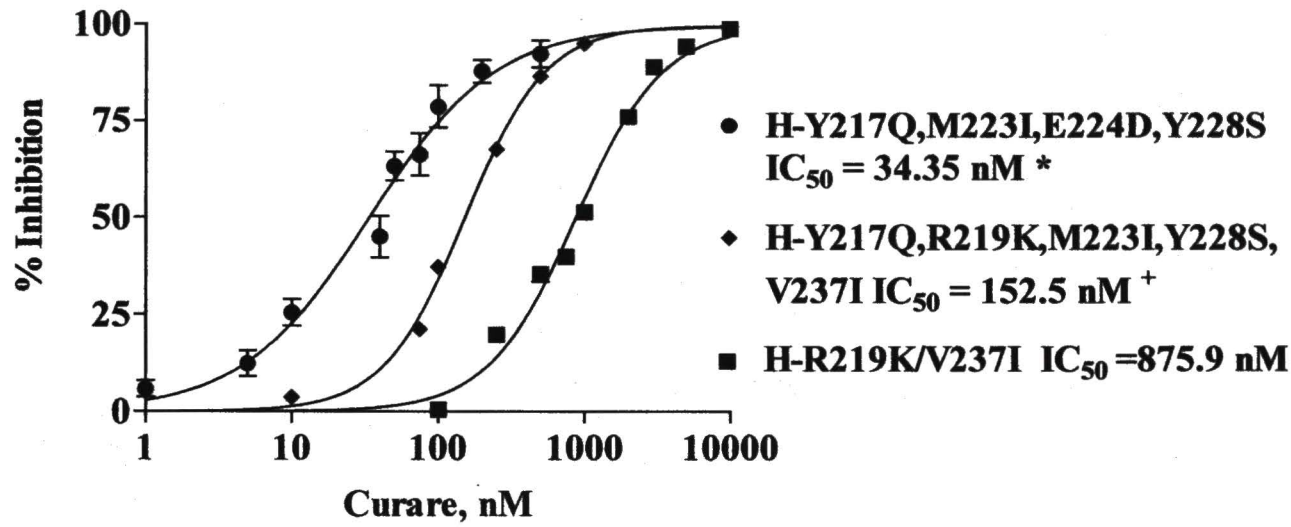

Figure 13 Curare inhibition response curves for H-2/3 Loop C receptor, H-R219K, V237I and H-Y217Q, R219K, M223I, Y228S, V237I. One-way ANOVA of IC_{50}s was significantly different, $F_{(2,44)} = 1079.2$, $p < 0.0001$; * $p < 0.05$, + $p < 0.001$ compared to H-2/3 Loop C, Tukey-Kramer post-hoc test. The interaction of R219K and V237I do not show any enhancement in the curare potency.

4. The differential curare sensitivity of heteromeric human and mouse (5-$HT_{3A/B}$) receptors.

The curare IC_{50} of the human heteromeric 5-HT_3 receptor (H-5-$HT_{3A/B}$) was reported to be 14.2 μM (Davies et al., 1999). While the curare IC_{50} of the rat heteromeric 5-HT_3 receptor was reported to be 27.6 nM (Hanna et al., 2000).

We constructed curare inhibition response curves for heteromeric mouse and human wild-type receptors ($5HT_{3A/B}$ receptors). This will set the stage for future work, i.e., investigation of the roles of Loop C and F in the process of ligand recognition in heteromeric receptors.

To ensure that subunit B is expressed along with subunit A of the $5HT_3$ receptor in *Xenopus* oocyte expression system, we tested the heteromeric mouse $5HT_3$ receptor (m-$5HT_{3A/B}$) with Picrotoxin a plant derived alkaloid which acts as an ion channel inhibitor. The heteromeric mouse $5HT_3$ receptor (5-$HT_{3A/B}$) is 100 fold less sensitive to Picrotoxin as compared to the homomeric mouse $5HT_3$ receptor (5-HT_{3A}) by whole cell patch clamp analysis (Das and Dillon, 2003). During our experiments we found approximately two fold difference between the Picrotoxin potencies in homomeric and heteromeric mouse $5HT_3$ receptors (Figure 13).

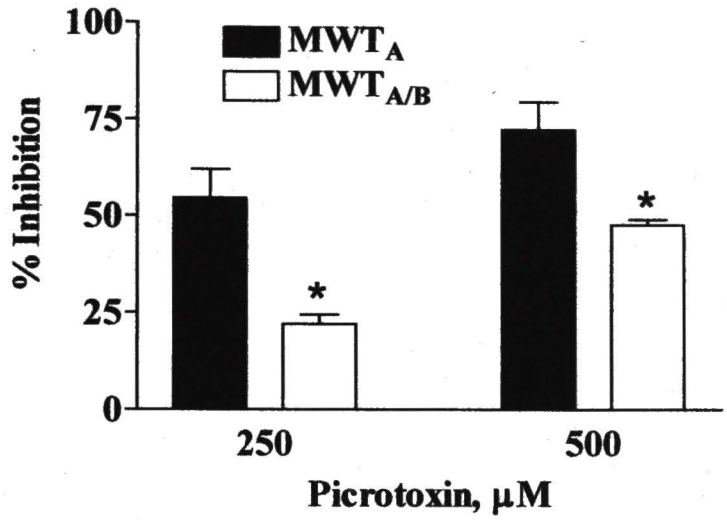

Figure 14 Picrotoxin inhibition in homomeric and heteromeric mouse $5HT_3$ receptors, (Student's paired t-test, $p, < 0.05$). MWT_A receptor shows greater % inhibition at 250 and 500 μM picrotoxin compared to the MWT_{A+B} receptor.

The curare IC_{50} was found to be 18.58±0.99 μM (Hill coefficient = 2.0±0.18) for heteromeric human 5-$HT_{3A/B}$ receptor and 0.115±0.004 μM (Hill coefficient = 1.0±0.04) for heteromeric mouse 5-$HT_{3A/B}$ receptor (Figure 14).

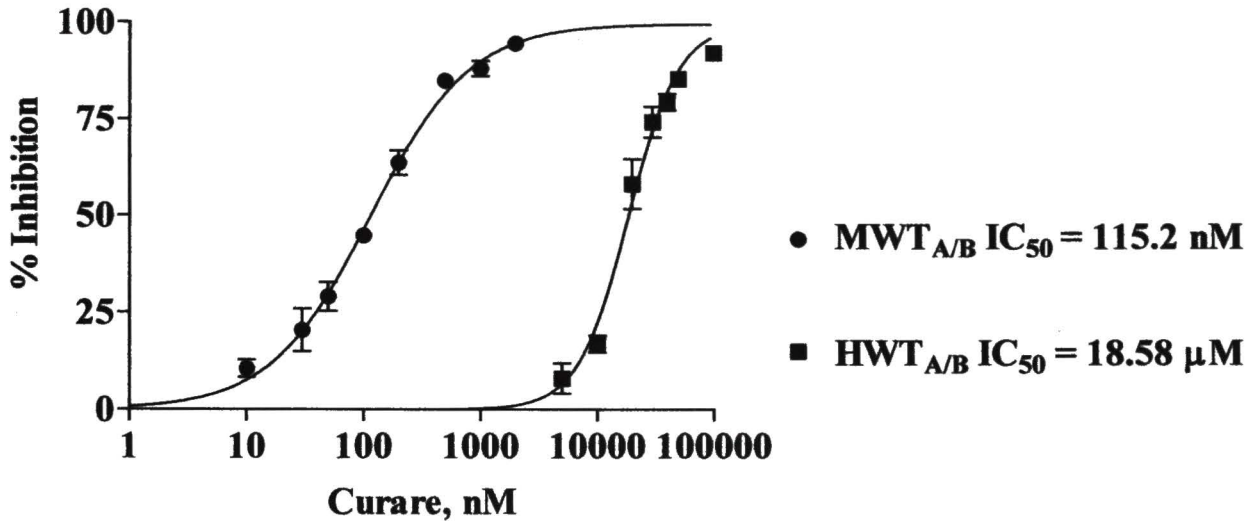

Figure 15 Curare inhibition response curves for heteromeric human and mouse receptors ($5HT_{3A/B}$). Heteromeric mouse $5HT_{3A/B}$ receptor shows approximately 100-fold higher curare potency as compared to the heteromeric human $5HT_{3A/B}$ receptor.

IV. DISCUSSION

The nicotinic acetylcholine receptor is a prototype of the ligand-gated ion channel superfamily, of which the 5-HT_3 receptor is a member. Domains contributing to the ligand-binding sites of the nACh receptor were identified by photoaffinity labeling, radio-ligand binding and ultrastructural studies (Sine et al., 2002). These studies provided a general overview for subsequent research with chimeric and point mutant receptor subunits. The pentameric composition of the receptor includes 2α, 1β, 1γ and 1δ or ε subunits. Binding occurs at the interface of two subunits, with α subunit containing the principal binding component and γ or δ subunit containing the complementary component. The principal binding component contains Loops A, B and C, while the complementary component contains Loops D, E and F. Based on its homology with ACHBP, it was demonstrated that the ligand-binding site of nACh receptor is composed of loops from the principal face of one subunit and a series of β strands from the complementary face of an adjacent subunit (Brejc et al., 2001).

Curare is a competitive antagonist for both the nACh receptor and 5-HT_3 receptor. At the nACh receptor, curare binds at the α-γ and α- δ subunit interfaces. It was observed that the structure activity relationships for curariform antagonists at mouse nACh receptor α/ γ subunit interface and mouse 5-HT_{3A} receptor subunit interface are broadly similar (Pedersen et al., 1995; Papineni et al., 1997; Yan et al., 1998). This suggests that the binding of curare at the 5-HT_{3A} receptor may also involve principal and complementary components. Similar to the nACh receptor, in the 5-HT_{3A} receptor, the

principal and complementary components belong to the opposite faces of adjacent subunits of the receptor. Loop C is a part of the principal component. The multiple non-conserved residues present in Loop C play a major role in determining the differential curare potency of the human and mouse 5-HT_{3A} receptors. Hope and co-workers (1999) constructed a human chimeric receptor in which the entire Loop C was replaced by corresponding mouse orthologs. The curare IC_{50} of this receptor was found to be 49.40 nM, which is much closer to the curare potency of the mouse wild-type 5-HT_{3A} receptor (curare IC_{50} = 1.40 nM) than that of the human wild-type 5-HT_{3A} receptor (curare IC_{50} = 2550 nM). This observation explains the contribution of Loop C in conferring the curare potency of the 5-HT_{3A} receptor (Hope et al., 1999). However, Loop C alone is not sufficient for conferring the curare potency of the receptor. Additional residues located elsewhere in the N-terminal domain also contribute in conferring the curare potency of the receptor (Hope et al., 1999).

Alignment of the N-terminal domains of mouse and human 5-HT_{3A} receptors reveals that all but three differences in Loops A-F are located in Loop C and F, which are located in the distal 1/3 region of the N-terminus. From the experiments conducted by a previous student in our laboratory, we know that the identity of distal 1/3 region of the extracellular N-terminal domain is sufficient to confer a curare potency of the 5-HT_{3A} receptor. In all, there are sixteen non-conserved residues present in the distal 1/3 region of N-terminal domains of mouse and human 5-HT_{3A} receptors. Of these residues, seven are present in Loop C, six are present in Loop F and three are present out side Loop C and F.

Although our laboratory has identified Loop F residues that contribute to curare potency of the 5-HT_{3A} receptors, it is clear that the role of Loop C residues is more complex. Previous studies in our laboratory demonstrated that a human 5-HT_{3A} receptor chimera containing Loop F mouse orthologs has a curare IC_{50} of 132 nM, while the human receptor chimera containing Loop C mouse orthologs (Hch Loop C receptor) has a curare IC_{50} of 41 nM. These results suggest that Loop C and Loop F play a redundant role in conferring the curare potency of the 5-HT_{3A} receptor. Previously, our laboratory identified two Loop F residues, when mutated to corresponding mouse orthologs, account for Loop F curare potency. This double mutant receptor H-K195, V202I has a curare IC_{50} of 134 nM. For this project, we decided to focus on Loop C and to report the roles of amino acid residues and their interactive effects on the ligand binding process.

For uniform comparison, a previous student constructed a human chimeric receptor, in which the entire Loop C domain was replaced by corresponding mouse orthologs (Hch Loop C receptor). The curare inhibition response curve for this receptor was constructed with an EC_{10} of 5-HT. The curare IC_{50} for this receptor was found to be 41 nM. To understand the effects of interactions of amino acid residues present in the Loop C region of the 5-HT_{3A} receptor, she tested several mini-chimeric receptors constructed on human background, containing four/five residues from Loop C region mutated to corresponding mouse orthologs. A chimeric receptor (H-2/3 Loop C receptor) containing four out of seven Loop C substituted residues, i.e., Y217Q, M223I, E224D and Y228S, was observed to have a curare IC_{50} of 34 nM. This result suggests that all mouse orthologs present in Loop C are not required to produce curare potency of Hch

Loop C receptor. From the previously collected data, we found that any random combination of four mouse orthologs present in Loop C region is not capable of producing a receptor with a curare IC_{50} of Hch Loop C receptor. For example, a human chimeric receptor containing four mutated Loop C residues (H-Y217Q, R219K, M223I, Y228S) had a curare IC_{50} of 100 nM. It is evident that exchange of R219K mutation with E224D produced a receptor with reduced curare potency. However, the E224D mutation by itself produces a rightward shift in the curare potency of the receptor (H-E224D curare IC_{50} = 8.9 μM). This suggests that the interaction of the aspartate residue with one or more mouse orthologs present in the H-2/3 Loop C receptor results in a curare IC_{50} of 34 nM. In addition, the E224D mutation may interact with additional mouse orthologs to enhance the curare potency. For example, the chimeric receptor H-M223I, E224D, S225I has a curare IC_{50} of 486 nM (Hope et al., 1999). In our laboratory we confirmed this result by constructing the H-M223I, E224D, S225I receptor. The curare IC_{50} for this receptor was found to be 284 nM.

Different researchers have stated the importance of this aspartate residue. It has been suggested that the aspartate residue present at 229th position in mouse 5-HT_{3A} receptor (which corresponds to 224th position in human 5-HT3A receptor) is in the close proximity with the ligand (Reeves et al., 2003) and is critical for 5-HT binding (Suryanarayanan et al., 2005). In the homology model proposed by Maksay and co-workers, this aspartate residue was reported to be involved in creating an acidic environment in the hydrophilic area of the binding pocket, which helps to attract the basic ligands. It was also suggested that this residue is one of the important contact point,

which forms a hydrogen bond with curare at the 7'OH group. Further, it was suggested that the serine residue at 225th position in the human 5-HT_{3A} receptor which is less bulky than the isoleucine residue present at 225th position in the mouse 5-HT_{3A} receptor, allows curare to move deep inside the binding cleft. That, along with the inability of 7'OH group to form hydrogen bond with glutamate residue (E224), is proposed to account for the lower curare potency of the human 5-HT_{3A} receptor (Maksay et al 2003).

Based on these findings, we hypothesized that E224D mutation must be present in combination with other mouse orthologs, in order to mimic the curare potency of Hch Loop C receptor. To verify this hypothesis, we constructed a human chimeric 5-HT_{3A} receptor in which five of the seven mutations of Hch Loop C receptor are present (E224D and V237I were excluded). This receptor, i.e., H-Y217Q, R219K, M223I, S225I, Y228S has a curare IC_{50} of 103 nM. We also observed that none of the chimeric receptors constructed on the background of H-5HT_{3A} receptor in our laboratory from which E224D mutation was excluded, had a curare IC_{50} of 34 nM. These results verify our hypothesis that the presence of E224D mutation is necessary in conferring the curare potency of Hch Loop C receptor. To determine whether all four mutations present in H-2/3 Loop C receptor are required to produce a curare IC_{50} of 34 nM, we tested several combinations of two or three point mutant residues for their curare potency. A previously constructed chimeric receptor H-Y217Q, M223I, Y228S has a curare IC_{50} of 175 nM. We also constructed four chimeric receptors on the human receptor background, namely H-M223I, E224D, Y228S (curare IC_{50} = 121 nM); H-Y217Q, M223I, E224D (curare IC_{50} = 457 nM); H-Y217Q, Y228S (curare IC_{50} = 353 nM) and H-M223I, E224D (curare IC_{50} = 1305 nM). Since none of these

receptors produced a curare IC_{50} of 34 nM, it is evident that all four mutations present in H-2/3 Loop C receptor are required.

The role of the S225I mutation in conferring curare potency was also explored. As mentioned previously, the curare potency of H-E224D was enhanced with the addition of two mouse orthologs: H-E224D (IC_{50} = 8.9 μM) < H-M223I, E224D (IC_{50} = 1.3 μM) < H-M223I, E224D, S225I (IC_{50} = 284 nM). While the addition of S225I mutation brings an approximately 4.5 fold enhancement in the curare potency of the three point mutant chimeric receptor, its addition to a chimeric receptor H-Y217Q, R219K, M223I, Y228S (IC_{50} = 100 nM), produced a chimeric receptor, H-Y217Q, R219K, M223I, S225I, Y228S with a curare IC_{50} of 103 nM. These results along with the results mentioned in the previous paragraph, suggests that more than one combinations of mouse Loop C orthologs can result in human chimeric 5-HT_{3A} receptor with curare $IC_{50} \leq 175$ and that S225I mutation is not required in any of them.

All but one of the subsets of mutations of the 2/3 Loop C chimeric receptor had greater curare potencies than the individual point mutant receptors comprising them. The rank order of curare potency of H-M223I, E224D, Y228S > H-Y217Q, Y228S > H-Y217Q, M223I, E224D > H-M223I, E224D > H-E224D suggests that Y228S has the greatest effect on the curare potency when combined with other mutations. To our knowledge this residue has not been implicated in ligand interactions in the 5-HT_{3A} receptors.

In combination with other mouse orthologs, the E224D mutation was found to be critical in conferring Loop C curare potency. However, it is not a general requirement for greater curare potencies among 5-HT_{3A} receptors that have been cloned from other mammalian species, such as rat and ferret (Mochizuki et al., 2000). Ferret and rat 5-HT_{3A} receptors contain a glutamate residue at the position corresponding to E224 in the human 5-HT_{3A} receptors (Figure 15) but have greater curare potency. The curare IC_{50} for ferret 5-HT_{3A} receptor was found to be 27 nM (Mochizuki et al., 2000) and the curare IC_{50} for rat 5-HT_{3A} receptor was found to be 32 nM (Mair et al., 1998). To explain this anomaly, we are planning to test the human triple mutant receptor containing rat or ferret orthologs at positions 223, 224 and 225. However, on the basis of presently available data, our assumption is that the other non-conserved amino acid residues present in Loop C as well as Loop F may play a role in conferring greater curare potency of rat and ferret 5-HT_{3A} receptors.

- 221 QFREFSLEDSSHYAEMKFYVV Ferret
- 217 YFREFSMESSNYYAEMKFYVV Human
- 221 KFQEFSIETSNSYAEMKFYVV Rat
- 220 QFKEFSIDISNSYAEMKFYVI Mouse

Figure 16 The sequential alignment of cDNAs encoding the 5-HT3A receptor subunits that have been cloned from ferret, human, rat and mouse. The E/D residues, which correspond to the critical E224, are shown in green.

Among the seven point mutant receptors previously constructed in our lab (Figure 7), the two receptors with highest curare potencies were H-R219K and H-V237I. However, the H-2/3 Loop C receptor with a curare potency of 34 nM does not contain either of these mutations. To test the effect of their presence in combination with other Loop C mutations, we constructed a chimeric receptor H-Y217Q, R219K, M223I, Y228S, V237I. The curare IC_{50} for this receptor was found to be 152.5 nM. Compared to the H-Y217Q, M223I, Y228S receptor (curare IC_{50} = 175 nM), this receptor does not show any significant change in the curare potency, suggesting that the interaction of R219K and V237I together, produces a minimal effect on the curare potency of Loop C. The curare IC_{50} of a minichimeric receptor H-R219K, V237I was found to be 875.9 nM, demonstrating a rightward shift in the curare potency as compared to the individual point mutant receptors. The 237th position in the human 5-HT_{3A} receptor is very close to the TM_1 domain and the V237I mutation may be involved in gating in addition to ligand binding. In H-V237I receptor, the isoleucine may alter the spatial orientation of Loop C, which facilitates curare binding with higher affinity. However, in the H-Y217Q, R219K, M223I, Y228S, V237I receptor, the interactions of other mouse residues with V237I, have a negative effect on the curare potency of the receptor, given that the four point mutant receptor chimera (H-Y217Q, R219K, M223I, Y228S) has a curare IC_{50} of 100 nM. Both Hch Loop C (containing all seven mutations) and H-217-> 228 receptor (containing six of the seven mutations) receptors have curare IC_{50}s of 40 nM and the difference between them is V237I mutation. Therefore the E224D and/or S225I

mutation(s) eliminate the negative effect of V237I mutation on the chimeric receptor potencies.

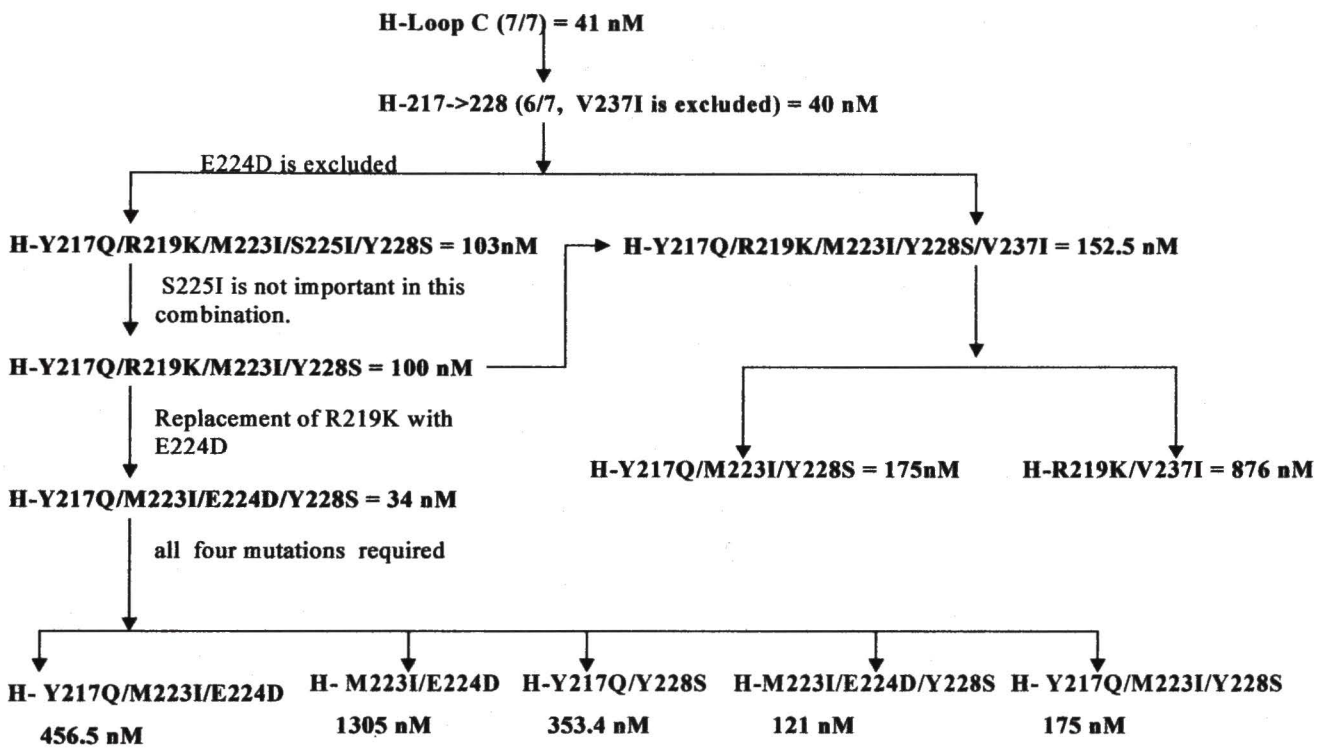

Figure 17 Summary of the roles of amino acid residues present in Loop C of the 5-HT_{3A} receptor, in the process of ligand binding.

The knowledge of interactive effects of amino acid residues present in Loop C is helpful for understanding the process of ligand recognition in 5-HT_{3A} receptors. However for a more thorough understanding of ligand-binding process in 5-HT_3 receptors, it is important to determine the amino acid residues involved in ligand binding process of

heteromeric 5-HT_3 receptors. We believe that the comparison of the curare potencies of the heteromeric mouse and human 5-HT_3 receptors will be a useful reference for future work. Similar experiments will be used to determine the contribution of the B subunit in conferring curare potency of the 5-$HT_{3A/B}$ receptors. As a first step we investigated heteromeric human and mouse 5-$HT_{3A/B}$ receptors in the *Xenopus* oocyte expression system in the two-electrode voltage clamp configuration. Given that there was a significant shift in the 5-HT concentration response curve in the human 5-$HT_{3A/B}$ receptor, we were confident of the expression of the heteromeric receptor. To ascertain the expression of the heteromeric mouse 5-$HT_{3A/B}$ receptor we compared the picrotoxin sensitivity of mouse wild-type 5-HT_{3A} and 5-$HT_{3A/B}$ receptors, and obtained similar findings to Das et al., 2003 in which picrotoxin was more potent in the homomeric receptor. In parallel to homomeric 5-HT_{3A} receptors, an approximately a 100 fold difference in the curare potency was also observed in the mouse and human 5-$HT_{3A/B}$ receptors. However, heteromeric 5-$HT_{3A/B}$ receptors activate and desensitize more quickly than homomeric 5-HT_{3A} receptors. Future studies of heteromeric receptors will be conducted in the HEK293 cell expression system in the whole cell patch clamp configuration, where solution exchange time will be much faster.

V. References:

1) Aapro M. S. 5-HT3 antagonists: an overview of their present status and further potential in cancer therapy-induced emesis. Drugs 42 (551-558), 1991.

2) Barrea Nelson P., Herbert Paul, Handerson Robert M., Martin Ian L. and Edwardson J. Michael. Atomic force microscopy reveals the stoichiometry and subunit arrangement of 5-HT3 receptors. PNAS 102 (12595-12600), 2005.

3) Beene D. L., Brandt G. S., Lester H.A. and Dougherty D. A. Cation-π Interactions in Ligand Recognition by Serotonergic (5-HT_{3A}) and Nicotinic Acetylcholine Receptors: The Anomalous Binding Properties of Nicotine. Biochemistry 41 (10262-10269), 2002.

4) Beene Darren L., Price Kerry L., Lester Henry L., Dougherty Dennis A. and Lummis Sarah C. R. Tyrosine residues that control binding and gating in the 5-hydroxytryptamine3 receptor revealed by unnatural amino acid mutagenesis. J. Neuroscience. 24(41): (9097-9104), 2004.

5) Belelli D., Balcareck J. M., Hope A. G., Peters J. A., Lambert J.J. and Blackburn T. P. Cloning and functional expression of human 5-Hydroxytryptamine type 3As receptor subunit. Molecular Pharmacology 48 (1054-1062), 1995.

6) Boyd Gary W., Low Pamela, Dunlop James I, Robertson Laura A., Vardy Audry, Lambert Jeremy J., Peters John A., and Connolly Christopher N.. Assembly and Cell Surface Expression of Homomeric and Heteromeric 5-HT3 Receptors: The

role of oligomerisation and Chaperone Proteins. Molecular and Cellular Neuroscience 21, (38-50), 2002.

7) Bouzat Cecilia, Gumilar1 Fernanda, Spitzmaul Guillermo, Wang Hai-Long, Rayes Diego, Hansen Scott B., Taylor Palmer and Sine Steven M. Coupling of agonist binding to channel gating in ACh-binding protein linked to an ion channel. Nature 430 (896-900), 2004.

8) Brady C. A., Stanford I. M., Ali I., Lin L., Williams J. M., Hope A. G., Dubin A. E. and Barnes N. M. Pharmacological comparison of human homomeric 5-HT3A receptors versus heteromeric 5-HT3A/3B receptors. Neuropharmacology 41 (282-284), 2001.

9) Brejc Katjusa, Dijk Willem J. van, Klaassen Remco V., Schuurmans Mascha, Oost John van der, Smit August B. and Sixma Titla K. Crystal structure of an ACh-binding protein reveals the ligand-binding domain of nicotinic receptors. Nature 411(6835) (269-276), 2001.

10) Dang H., England P. M., Farivar S. S., Doughrty D. A. and Lester H. A. Probing the role of a conserved M1 Proline residue in 5-Hydroxytryptamine3 Receptor Gating. Molecular Pharmacology 57 (1114-1122), 2000.

11) Das Paromita and Dillon G. H. The 5-HT3B subunit confers reduced sensitivity to picrotoxin when co-expressed with the 5-HT3A receptor. Molecular Brain Research 119 (207-212), 2003.

12) Davies P.A., Pistis M., Hanna M. C., Peters J. A., Lambert J. J., Hales T. G. and Kirkness E. F. The 5-HT3B subunit is a major determinant of serotonin-receptor function. Nature 397 (359-363), 1999.

13) Dubin A.E, Huvar R., D'Andreas M. R., Pyati J., Zhu J. Y., Koy K. C., Wilson S. J., Galindo J. E., Glass C. A., Lin L., Jackson M. R., Lovenberg T. W. and Erlander M. G. The pharmacological and functional characteristics of the serotonin 5-HT (3A) receptor are specifically modified by a 5-HT(3B) receptor subunit. J. Biol. Chem. 274 (30799), 1999.

14) Eisele J.L., Bertrand S., Galzi J.L., Deillers-Thiery A., Chageux J. P., and Bertrand D. Chimaeric nicotinic-serotonergic receptor combines distinct ligand binding and channel specificities. Nature336 (479-483), 1993.

15) Galzi J.L. and Changeux J.P. Neuronal nicotinic receptors: molecular organization and regulations. Neuropharmacology 34 (563-582), 1995.

16) Gelhert D. R., Gackenheimer S. L., Wong D. T., and Robertson D. W. Localization of 5-HT3 receptors in the rat brain using ^{3}[H]-LY278584. Brain research 553 (149-154), 1991.

17) Hapfelmeir G., Tredt C., Haseneder R., Zeiglgansberger W., Eisensamer B., Ruppercht R., and Rammes G. Co-expression of the 5-HT3B Serotonin receptor subunit alters the biophysics of the 5-HT3 receptor. Biophysical J. 84(3): 1720-33, 2003.

18) Hanna Michael C., Davis Paul C., Hales Tim G. and Kirkness Ewen F.. Evidence for expression of heteromeric serotonin 5-HT (3) receptors in rodents. J. Neurochem. 75(1) (240-247), 2000.

19) Hayrapetyan V., Jenschke M., Dillon G. H. and Machu T. K. Co-expression of the 5-HT3B subunit with the 5-HT3A receptor reduces alchohol sensitivity. Molecular Brain Research 142 (146-150), 2005.

20) Hope Anthony G., Belelli Delia, Mair Ian D., Lambert Jeremy J. and Peters John A. Molecular determinants of (+)-tubocurarine binding at recombinant 5-hydroxytryptamine3A receptor subunits. Mol. Pharmacology 55 (1037), 1999.

21) Ilegelms Erwin, Pick Horst M., Deluz Cedrick, Kellenberger Stephen and Vogel Horst. Noninvasive Imaging of 5-HT3 receptor Trafficking in Live Cells. Journal of Biological Chemistry 279 (53346-53352), 2004.

22) Im W. B., Pregenzer J. F., Binder J. A., Dillon G. H. and Alberts G. L. Chloride Channel Expression with the Tandem Construct of α6-β2 GABAA receptor subunit Requires a Monomeric subunit of α6 or γ2*. Journal of Biological Chemistry 270 (26063-26066), 1995

23) Johnson B. A., Campling G. M., Griffith P. and Cohen P. J. Attenuation of some alcohol-induced mood changes and the desire to drink by 5-HT3 receptor blockade: A preliminary study in healthy male volunteers. Psychopharmacology 112 (142-144), 1993.

24) Johnson B. A., Roache J. D., Javors M. A., DiClemente C. C., Prihoda T. J., Cloninger C. R., Brodnick P. S., Ait-Daoud N. and Hensler J. Ondansetron for

reduction of drinking among biologically predisposed alcoholic patients: A randomized control trial. JAMA 284 (963-971), 2000.

25) Kash T. L., Jenkins A., Kelley J. C., Trudell J. R. and Harrison N. L. Coupling of agonist binding to channel gating in GABA(A) receptor. Nature 421 (272-275), 2003.

26) Kawa K.. Distribution and functional properties of 5-HT3 receptors in the rat hippocampal dentate gyrus: a patch-clamp study. J.Neurophysiology.71 (5) (1935-1947), 1994.

27) Knapp D.J. and Pohorecky L. A. Zacopride, a 5-HT3 receptor antagonist, reduces voluntary ethanol consumption in rats. Pharmacol. Biochem. And Behav. 41 (847-850), 1992.

28) Kash Thomas A., Jenkins Andrew, Kelley Jill C., Trudell James R. Coupling of agonist binding to channel gating in the GABAA receptor. Nature 421 (272-275), 2003.

29) Lambert J.J., Peters J. A., Hales T. G., Dempster J. The properties of 5-HT3 receptors in clonal cell lines studied by patch-clamp techniques Br. J. Pharmacology 97 (27-40), 1989.

30) Lankeiwicz S., Lobitz N., Wetzel C. H. R., Ruppercht R, Gisselmann G. Molecular cloning, functional expression, and pharmacological characterization of 5-hydroxytryptamine3-receptor cDNA and its splice variants from guinea pig. Mol. Pharmacology. 53 (202-212), 1998.

31) Lummis S. C., Beene D. L., Lee L. W., Lester H. A., Broadhurst R. W. and Dougherty D. A. *Cis-trans* isomerization at a proline opens the pore of neurotransmitter-gated ion channel. Nature 438 (248-252), 2005.

32) Maksay G., Bikadi Z., Simonyi M. Binding Interactions of Antagonists with 5-Hydroxytryptamine3A Receptor Models. Journal of Receptors and Signal Transduction 23 (255-270), 2003.

33) Maricq A.V., Peterson A. S., Brake A. J., Myres R. M. and Julias D. Primary structure and functional expression of the 5HT3 receptor, a serotonin-gated ion channel. Science 154: 432-437, 1991.

34) Miquel M.C., Emerit M. B., Gingrich J. A., Nosjean A., Hamon M. and Mestikawy S. E. Developmental changes of the differential expression of two serotonin 5-HT3 receptor splice variants in rat. Journal of Neurochemistry 65 (475-483), 1995.

35) Miyake A. Molecular cloning of human 5-Hydroxytryptamine3 receptors: heterogeneity in distribution and function among species. European Journal of Pharmacology 48 (407-416), 1995.

36) Mochizuki S., Miyake A. and Furuichi K. Identification of a domain affecting agonist potency of meta-chlorophenyl biguanide in 5-HT3 receptors. Eur. J. Pharmacology. 369 (125-132), 1999.

37) Monk Sarah A., Williams Julie M., Hope Anthony G. and Barnes Nicholas M. Identification and importance of N-glycosyalation of the human 5-

Hydroxytryptamine3A receptor subunit. Biochemical Pharmacology 68 (1787-1796), 2004.

38) Niesler Beate, Frank Bernd, Kapeller Johannes, Rappold Gudrun A. Cloning, physical mapping and expression analysis of the human 5-HT3 serotonin receptor-like genes HTR3C, HTR3D and HTR3E*. GENE 310 (101-111), 2003.

39) Peters J. A. Molecular determinants of single channel conductance and ion selectivity in the Cys-loop family: insights from the 5-HT3 receptor. *TRENDS* in Pharmacological Sciences 26 (587-593), 2005.

40) Price Kerry L. and Lummis Sarah C. R. The role of tyrosine residues in the extracellular domain of the 5-hydroxytryptamine3 receptor. J. Bio. Chem. 279(22) (23294-23301), 2004.

41) Quirk Phillip L., Rao Suma, Roth Bryan L., and Siegelg Ruth E. Three Putative N-Glycosylation Sites Within The Murine 5-HT3A Receptor Sequence Affect Plasma Membrane Targeting, Ligand Binding and Calcium Influx in Heterologus Mammalian Cells. Journal of Neuroscience Research 77 (498-506), 2004.

42) Reeves David C. and Lummis Sara C. R. The molecular basis of the structure and function of the 5-HT3 receptor: a model ligand-gated ion channel (review). Mol. Memb. Bio. 19(1) (11-26), 2002.

43) Reeves David C., Sayed Muhammad F. R., Chau Pak-Lee, Price Kerry L. and Lummis Sarah C. R. Prediction of 5-HT3 Receptor Agonist-Binding Residues using Homology Modeling. Biophysical Journal 84 (2338-2344), 2003.

44) Reeves D.C., Jansen M., Bali M., Lemster T., Akabas M. H. A Role for the β1-β2 Loop in the Gating of 5-HT3 Receptors. Journal of Neuroscience 25 (9358-9366), 2005.

45) Schreiter Christoph, Hovius Ruud, Costioli Matteo, Pick Horst, Kellenberger Stephan, Schild Laurent and Vogel Horst. Characterization of the Ligand-Binding site of the Serotonin 5-HT3 Receptor. THE ROLE OF GLUTAMATE RESIDUES 97, 224 AND 235*. Journal of Biological Chemistry 278 (22709-22716), 2003.

46) Speir A.D., and Lummis S. C. The role of tryptophan residues in the 5-Hydroxytryptamine(3) receptor ligand binding domain. Journal of Biological Chemistry. 275 (5620-5625), 2000.

47) Stevens R., Rusch D., Solt K., Raines D. E., Davies P. A. Modulation of Human 5-Hydroxytryptamine Type 3AB Receptors By Volatile Anesthetics and *n*-Alcohols. The Journal of Pharmacology and Experimental Therapeutics 314 (338-345), 2005.

48) Suryanarayanan Asha, Joshi Prasad R., Bikadi Zsolt, Mani Muthalagi, Kulkarni Trupti R., Gaines Chandra and Schulte Marvin K. The Loop C region of the Murine 5-HT3A receptor contributes to the Differential Actions of 5-Hydroxytryptamine and *m*-chlorophenylbiguanide Biochemistry 44 (9140-9149), 2005.

49) Swift R. M., Davidson D., Welihan W. and Kuzentsov O. Ondansetron alters human alcohol intoxication. Biol. Pschy. 40 (514-521), 1996.

50) Thompson Andrew J., Price Kerry L., Reeves David C., Chan S. Ling, Chau P.-L. and Lummis Sarah C. R. A single ring of charged amino acids at one end of the pore can control ion selectivity in the 5-HT3 receptor. British Journal of Pharmacology 140 (359-365), 2003.

51) Tairi A. P., Hovus R., Pick H., Blasey H., Bernard A., Surprenant A., Lundstorm K. and Vogel H. Ligand binding to the serotonin 5HT3 receptor studied with a novel fluorescent ligand. Biochemistry 37 (15850-15864), 1998.

52) Tyeres M. B. 5-HT3 receptors and the therapeutic potential of 5-HT3 antagonist. *Therapie* 46 (431-435), 1991.

53) Yakel J.L. and Jackson M. B. 5-HT3 receptors mediate rapid responses in cultured hippocampus and a clonal cell line. Neuron. Neuron1 (615-621), 1988.

54) Yan Dong and White Michael. Interaction of *d*-tubocurarine analogs with mutant 5-HT3 receptors. Neuropharmacology 43 (367-373), 2002.

55) Yan D., White M. M. Spatial orientation of the Antagonist Granisetron in the Ligand-Binding site of the 5-HT3 Receptor. Molecular Pharmacology 68 (365-371), 2005.